

Supporting Information

Preparation and properties of multifunctional phenoxyacetate-based ionic liquids and their application in citrus bacteriostatic preservation

Yifei Zhou, Qiuxiao Wang, Tao Wang, Haixiang Gao*

Department of Applied Chemistry, China Agricultural University

Yuanmingyuan West Road 2#, Haidian, Beijing, 100193, Peop. Rep. China.

E-mail: hxgao@cau.edu.cn

Table S1. Solubility of water at different pH

Compound	Solubility of water at different pH (mg/L)		
	5.0	7.0	9.0
Free acid sodium	>10 ⁵	>10 ⁵	>10 ⁵
2,4-D	407.90	870.29	1117.39
DIL-1	2962.11	2037.55	1850.94
DIL-2	3878.48	2757.12	1953.97
DIL-3	238.55	232.39	238.69
4-CPA	402.83	982.20	1301.74
CIL-1	1230.18	1233.65	1366.50
CIL-2	3348.28	3217.76	2190.85
CIL-3	74.16	251.43	206.90
MCPA	321.68	894.87	1071.56
MIL-1	2676.98	1848.48	1909.03
MIL-2	1380.52	1047.74	836.50
MIL-3	31.45	202.72	157.64
PAA	4540.87	5853.71	5867.12
PIL-1	2107.86	2087.39	1991.93
PIL-2	5195.92	4464.82	7069.45
PIL-3	1030.23	468.73	758.63

Table S2. Fungicidal Activities of free acids and alkaloids and fungicides against different fungi

Fungi	2,4-D	4-CPA	MCPA	PAA	PAL	GRA	PYR	PRO
Pythium	-1.95%	2.92%	5.11%	10.22%	1.53%	1.75%	5.68%	96.94%
Rhizoctonia	0.44%	-0.65%	0.22%	4.14%	29.91%	1.34%	59.15%	0.22%
Phytophthora	8.26%	4.59%	15.37%	-0.69%	78.04%	-1.67%	99.05%	31.26%
S. Sorauer	14.25%	2.57%	11.45%	5.14%	41.84%	27.19%	83.69%	6.38%
Cytospora sp.	-0.23%	-3.20%	7.31%	-1.83%	0.68%	-1.37%	19.18%	-1.14%
B. cinerea	0.24%	5.67%	6.86%	-4.02%	6.56%	1.09%	84.90%	0.66%
S. sclerotiorum	-1.44%	4.09%	5.29%	-5.77%	5.44%	3.07%	75.89%	0.71%
F. graminearum	0.89%	1.33%	0.67%	-1.11%	30.67%	10.67%	24.00%	6.67%
P. citrinum	1.19%	1.43%	1.43%	2.39%	7.16%	3.10%	85.20%	0.24%

Table S3. Fungicidal Activities of the PILs against different fungi

	Pythium	Rhizoctonia	Phytophthora	S. Sorauer	Cytospora sp.	B. cinerea	S. sclerotiorum	F. graminearum	P. citrinum
DIL-1	8.81%	28.32%	72.99%	34.93%	29.33%	10.27%	7.28%	64.47%	17.97%
DIL-2	7.49%	13.27%	7.11%	65.07%	17.07%	28.35%	3.75%	46.27%	13.00%
DIL-3	11.89%	63.05%	97.63%	94.06%	59.62%	78.35%	99.12%	59.87%	88.18%
DIL-4	98.90%	15.27%	51.42%	25.57%	10.10%	17.19%	6.18%	50.00%	9.22%
CIL-1	7.05%	26.55%	69.67%	43.38%	18.27%	10.94%	3.75%	58.99%	17.97%
CIL-2	5.73%	15.93%	3.79%	9.82%	10.82%	23.88%	2.43%	32.46%	52.72%
CIL-3	10.13%	48.78%	97.39%	91.57%	34.16%	91.19%	98.21%	52.41%	85.82%
CIL-4	98.24%	73.89%	76.78%	96.35%	73.80%	95.98%	91.61%	49.12%	10.64%
MIL-1	5.73%	25.44%	71.09%	34.70%	41.83%	20.76%	20.97%	59.87%	32.05%
MIL-2	11.45%	6.26%	0.24%	31.15%	18.74%	33.48%	10.76%	36.67%	13.49%
MIL-3	14.98%	99.57%	98.10%	88.52%	62.98%	91.19%	96.41%	52.89%	85.54%
MIL-4	96.48%	4.97%	22.99%	25.53%	14.45%	27.97%	63.90%	36.89%	12.29%
PIL-1	5.51%	25.27%	71.56%	33.96%	19.41%	-0.44%	13.68%	51.56%	20.72%
PIL-2	9.25%	7.99%	-5.92%	13.11%	1.13%	1.32%	9.19%	38.67%	14.22%
PIL-3	12.33%	98.70%	99.05%	93.44%	33.18%	55.29%	90.81%	41.78%	87.95%
PIL-4	94.49%	6.26%	15.17%	16.39%	2.48%	3.74%	76.46%	37.11%	9.88%

Table S4. Efficacy test of DIL-3 on citrus

	Incidence (%)	Disease index (%)	Relative control effect (%)
DIL-3	10%	2.5%	88.89%
2,4-D	30%	22.5%	62.5%
CK	80%	60.0%	

Table S5. Standard curves of ionic liquids

	Standard curve	R ²
2,4-D	$y = 0.0354x + 0.0922$	0.9967
DIL-1	$y = 0.0496x - 0.0372$	0.9996
DIL-2	$y = 0.0216x - 0.0324$	0.9999
DIL-3	$y = 0.0179x - 0.0118$	0.9993
DIL-4	$y = 0.0239x + 0.0179$	0.9998
4-CPA	$y = 0.0432x + 0.1997$	0.9957
CIL-1	$y = 0.0587x - 0.0331$	0.9995
CIL-2	$y = 0.0356x + 0.2239$	0.9911
CIL-3	$y = 0.0183x + 0.0118$	0.9987
CIL-4	$y = 0.0292x + 0.0742$	0.9945
MCPA	$y = 0.0437x + 0.0333$	0.9977
MIL-1	$y = 0.0612x - 0.0159$	0.9999
MIL-2	$y = 0.0395x - 0.0748$	0.9957
MIL-3	$y = 0.0395x - 0.0748$	0.9999
MIL-4	$y = 0.0281x + 0.0724$	0.9989
PAA	$y = 0.0379x + 0.1289$	0.9981
PIL-1	$y = 0.0796x - 0.0241$	0.9997
PIL-2	$y = 0.051x + 0.1768$	0.9932
PIL-3	$y = 0.1087x + 0.0507$	0.9995
PIL-4	$y = 0.0204x + 0.0774$	0.9997

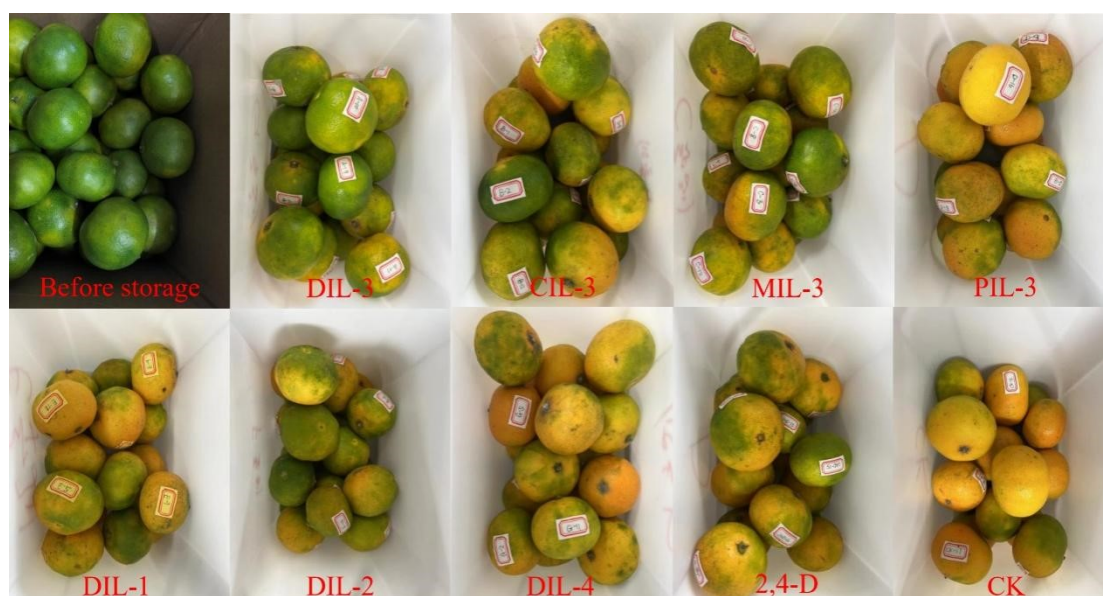


Figure S1. Comparison photos of citrus after 20 days of storage and before storage.

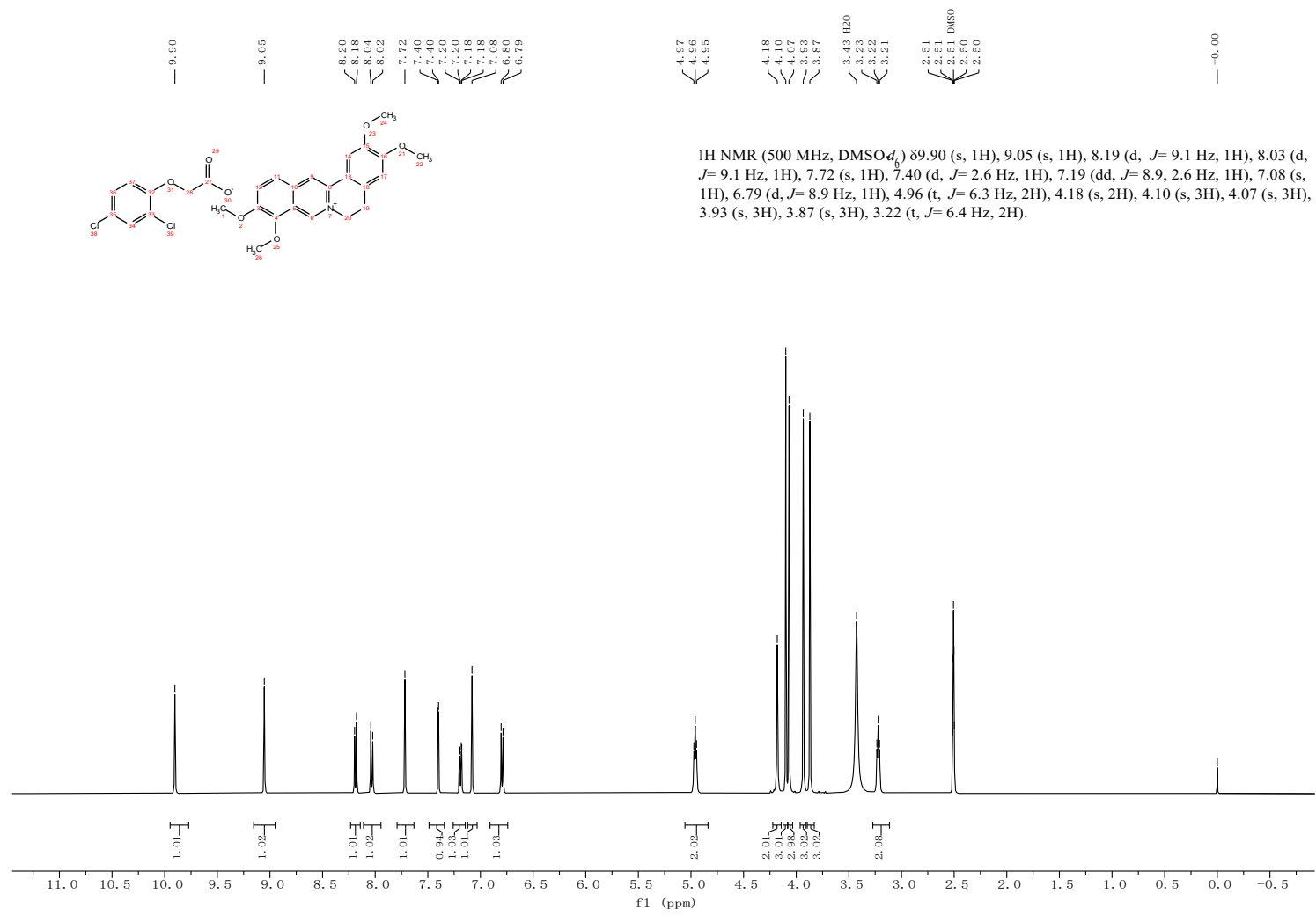


Fig. S2 ¹H NMR (500 MHz; DMSO-d₆; Me₄Si) of DIL-1 (2-(2,4-dichlorophenoxy)acetate 2,3,9,10-tetramethoxy-5,6-dihydroisoquinolino[3,2-a]isoquinolin-7-ium)

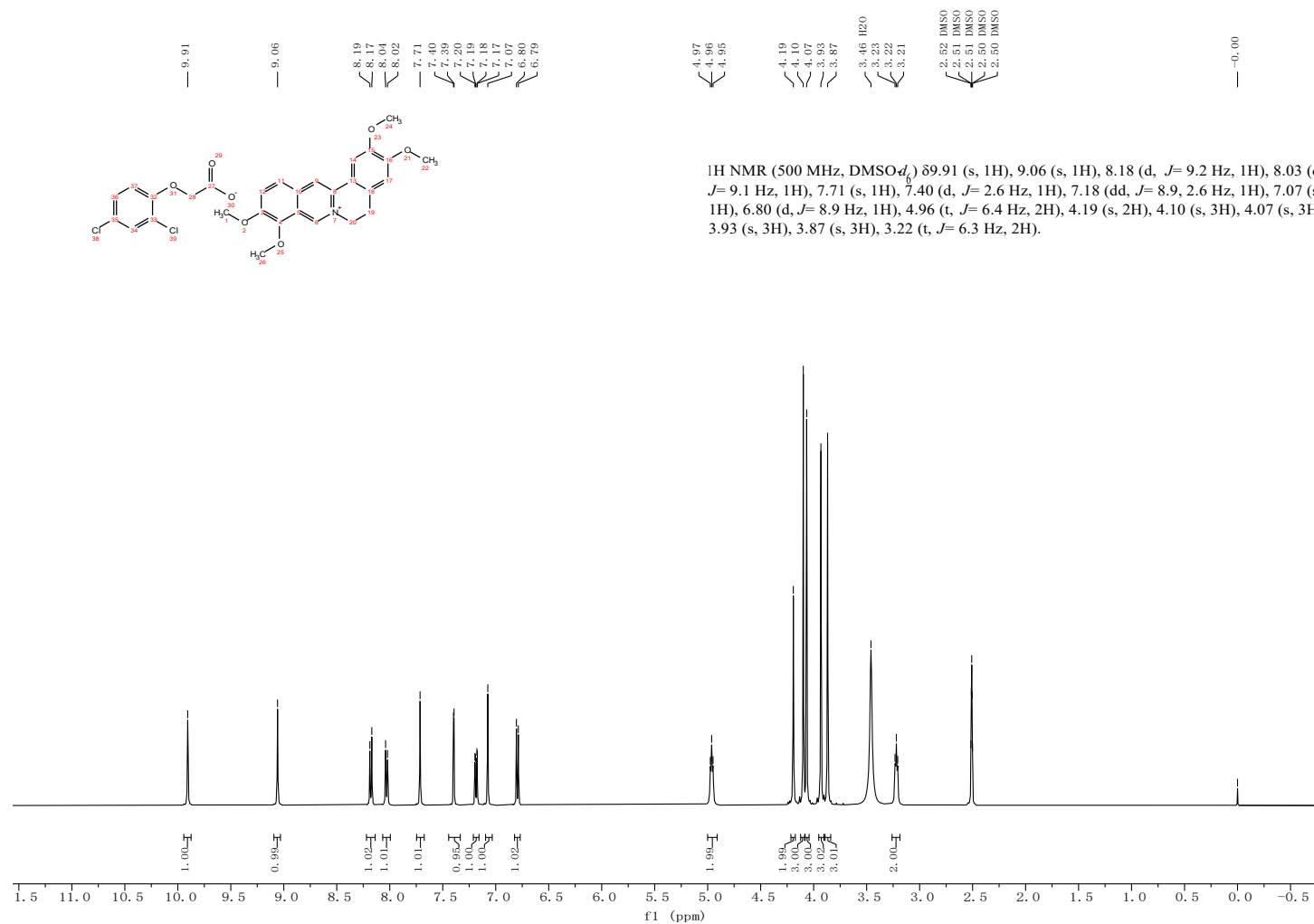


Fig. S3 $^1\text{H NMR}$ (500 MHz; $\text{DMSO-}d_6$; Me_4Si) of DIL-1 after volatility test

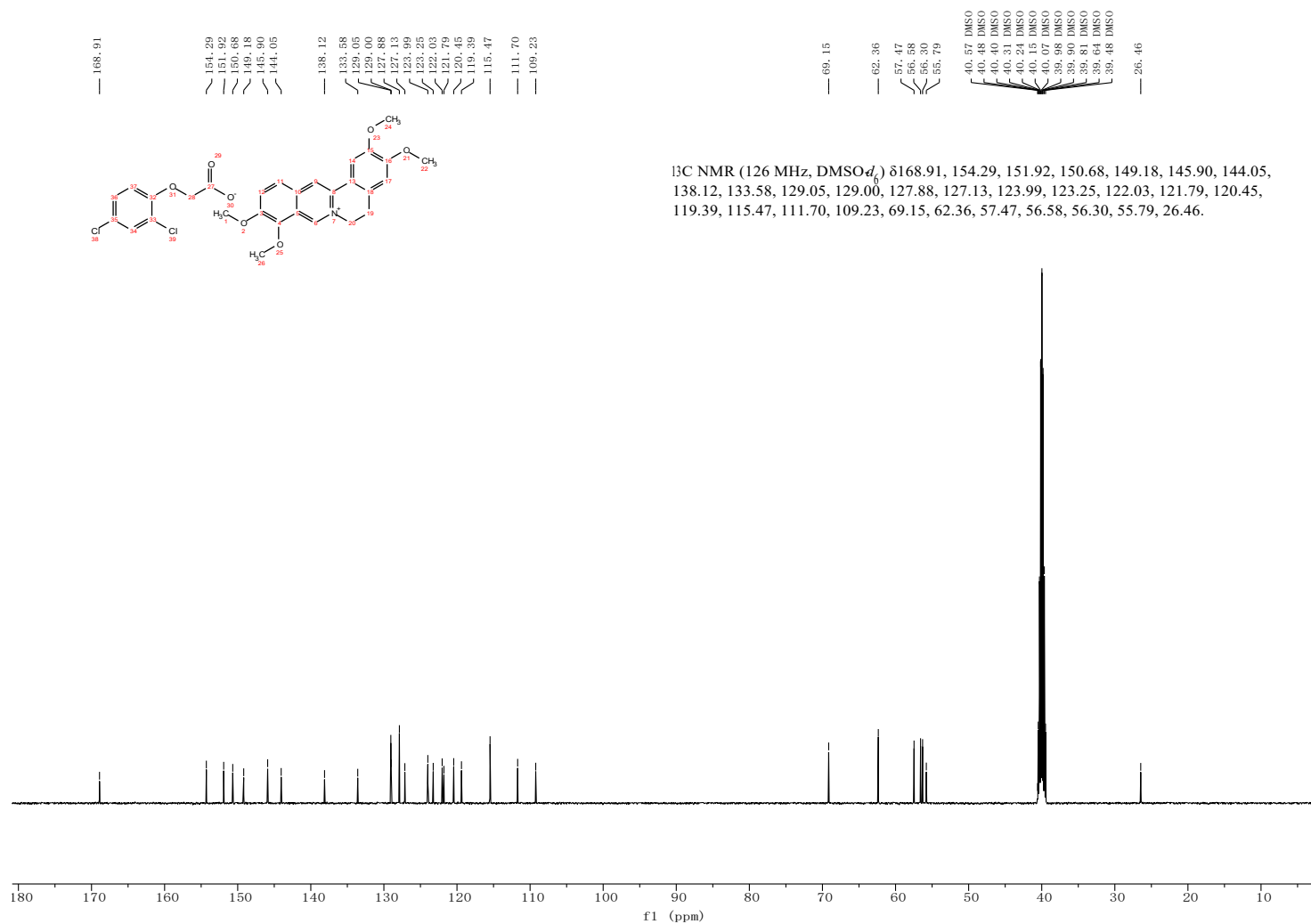


Fig. S4 ^{13}C NMR (126 MHz; $\text{DMSO}-d_6$; Me_4Si) of DIL-1 (2-(2,4-dichlorophenoxy)acetate 2,3,9,10-tetramethoxy-5,6-dihydroisoquinolino[3,2-a]isoquinolin-7-ium)

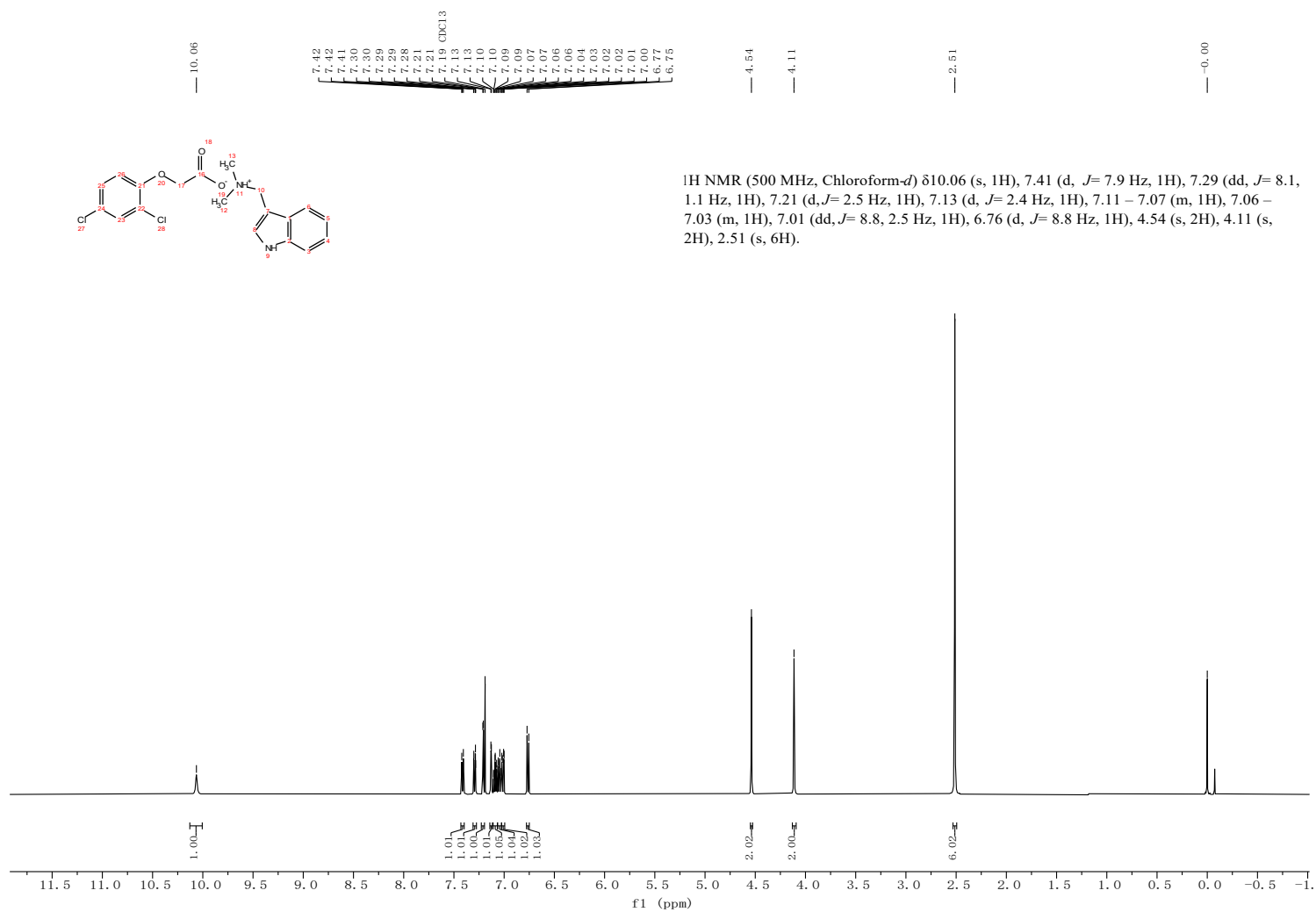


Fig. S5 ¹H NMR (500 MHz; CDCl₃; Me₄Si) of DIL-2 (2-(2,4-dichlorophenoxy)acetate 1-(1H-indol-3-yl)-N,N-dimethylmethanaminium)

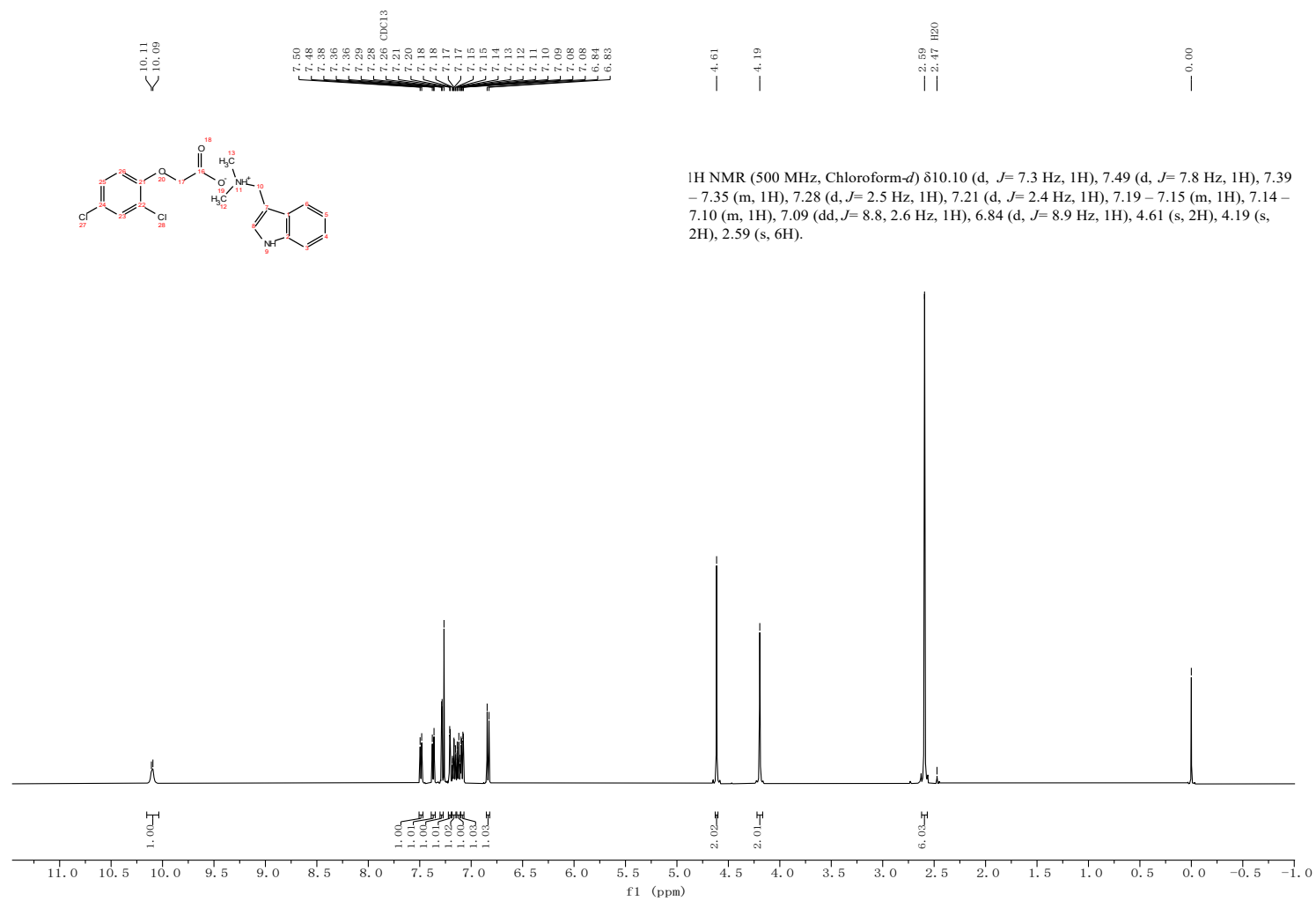


Fig. S6 ¹H NMR (500 MHz; CDCl₃; Me₄Si) of DIL-2 after volatility test

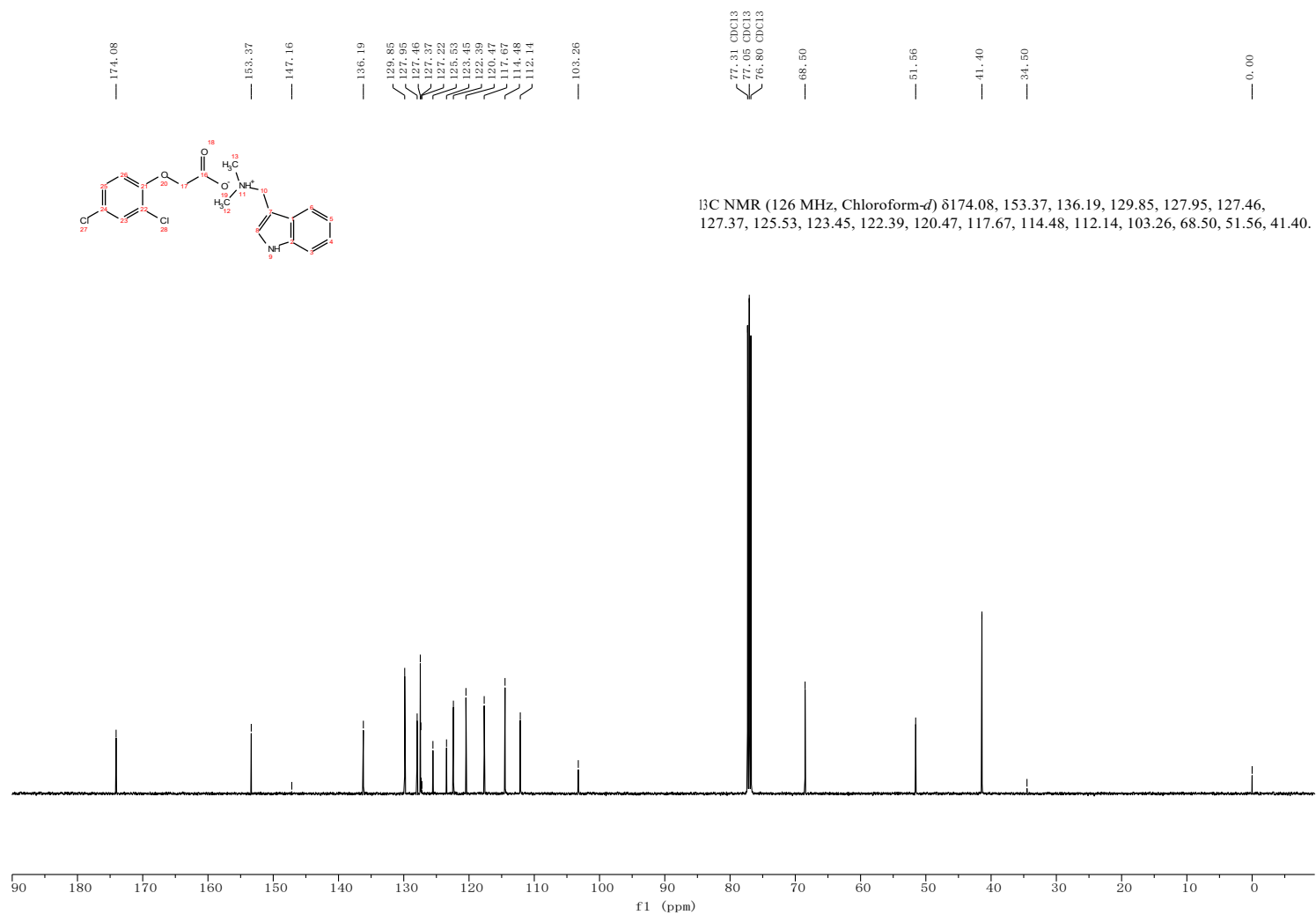


Fig. S7 ¹³C NMR (126 MHz; CDCl₃; Me₄Si) of DIL-2 (2-(2,4-dichlorophenoxy)acetate 1-(1H-indol-3-yl)-N,N-dimethylmethanaminium)

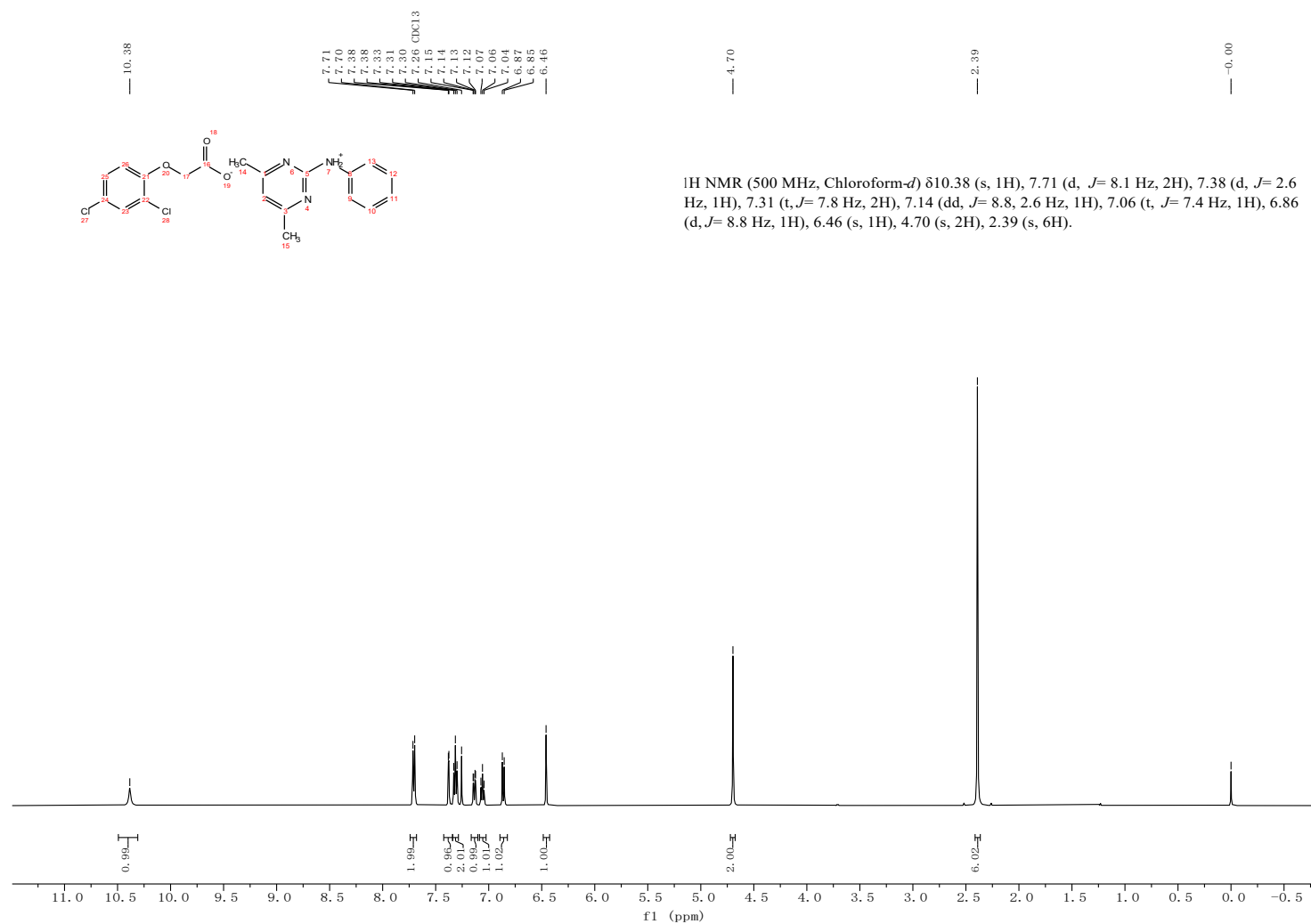


Fig. S8 ¹H NMR (500 MHz; CDCl₃; Me₄Si) of DIL-3 (2-(2,4-dichlorophenoxy)acetate 4,6-dimethyl-N-phenylpyrimidin-2-aminium)

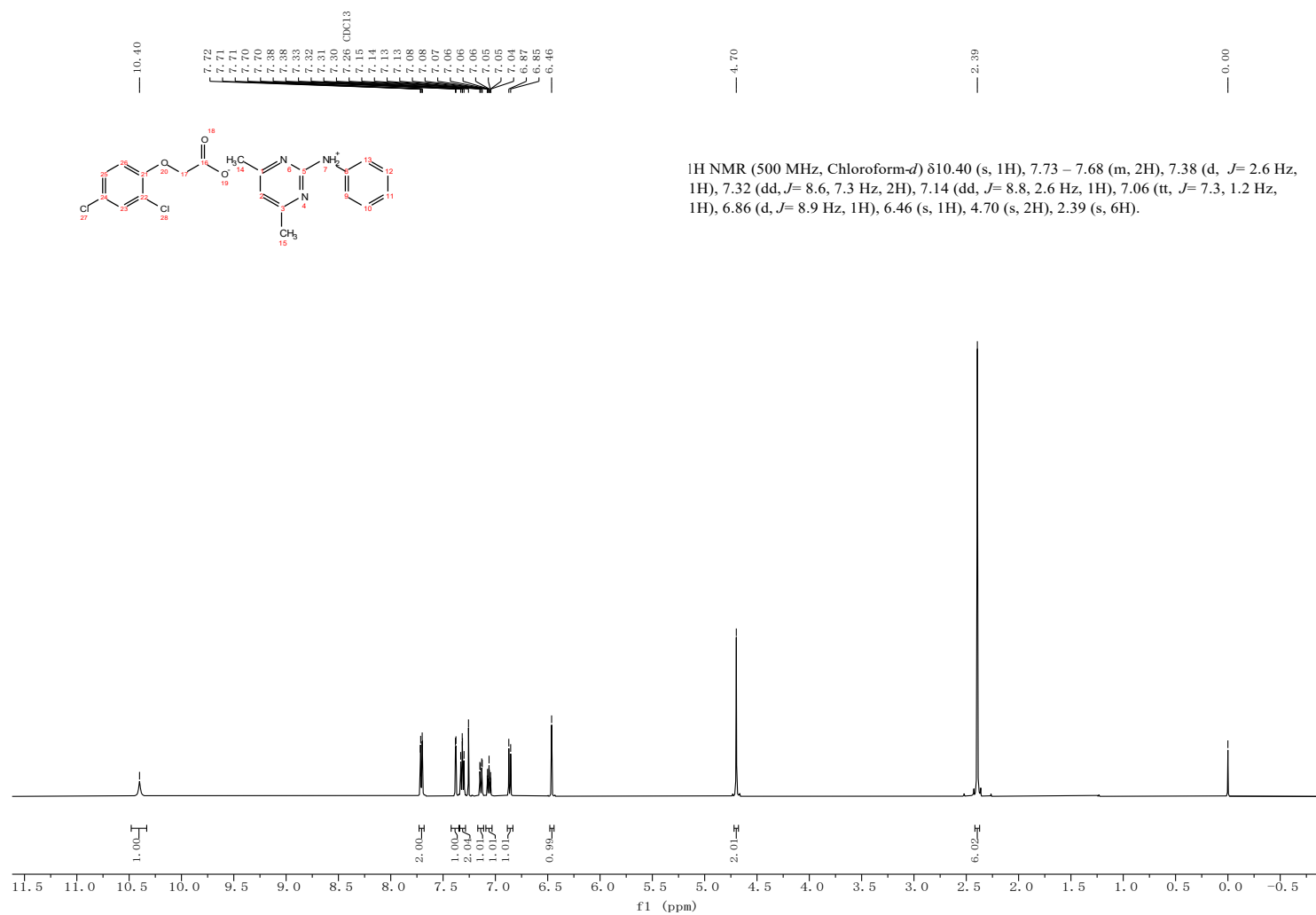


Fig. S9 ¹H NMR (500 MHz; CDCl₃; Me₄Si) of DIL-3 after volatility test

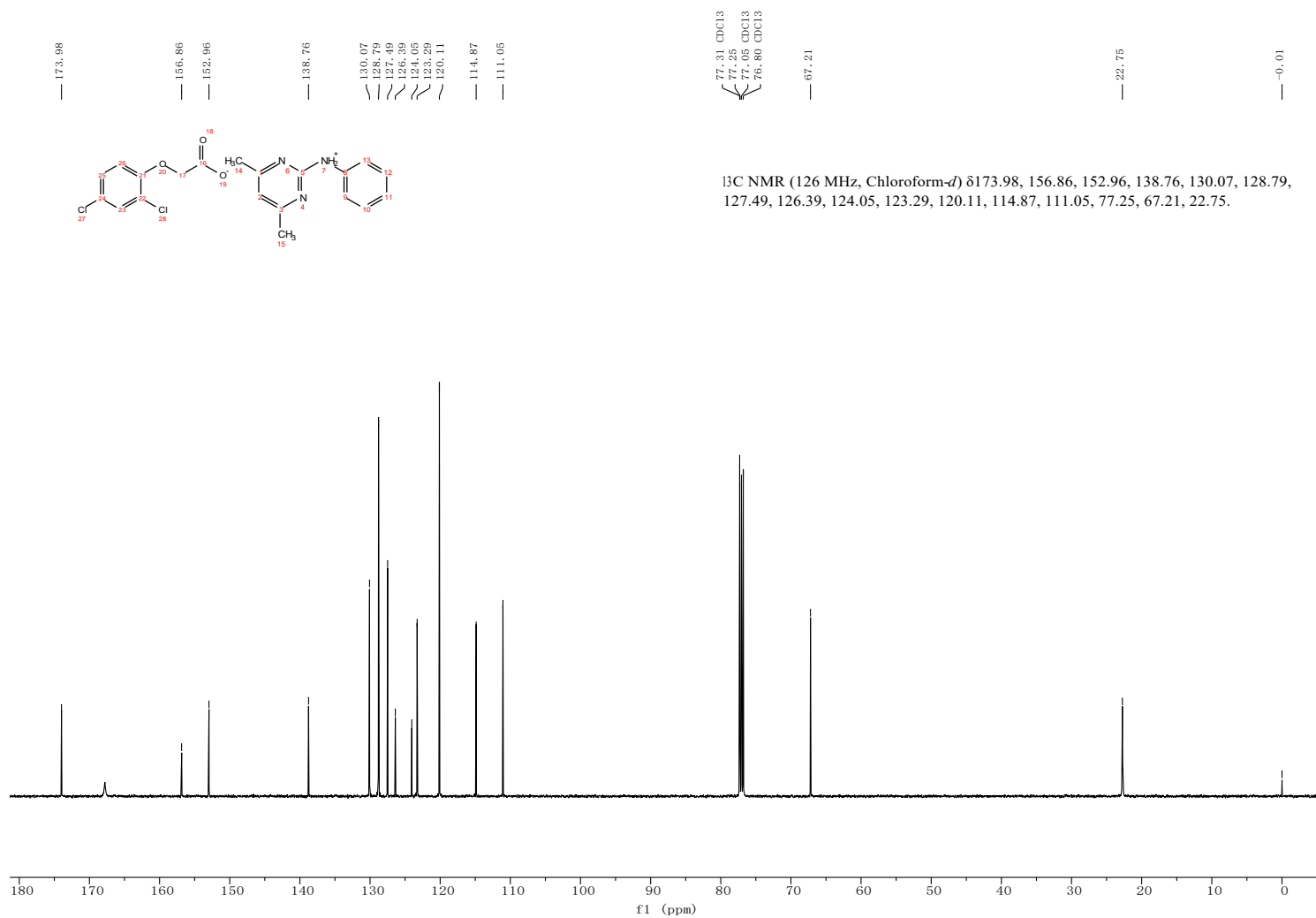


Fig S10 ¹³C NMR (126 MHz; CDCl₃; Me₄Si) of DIL-3 (2-(2,4-dichlorophenoxy)acetate 4,6-dimethyl-N-phenylpyrimidin-2-aminium)

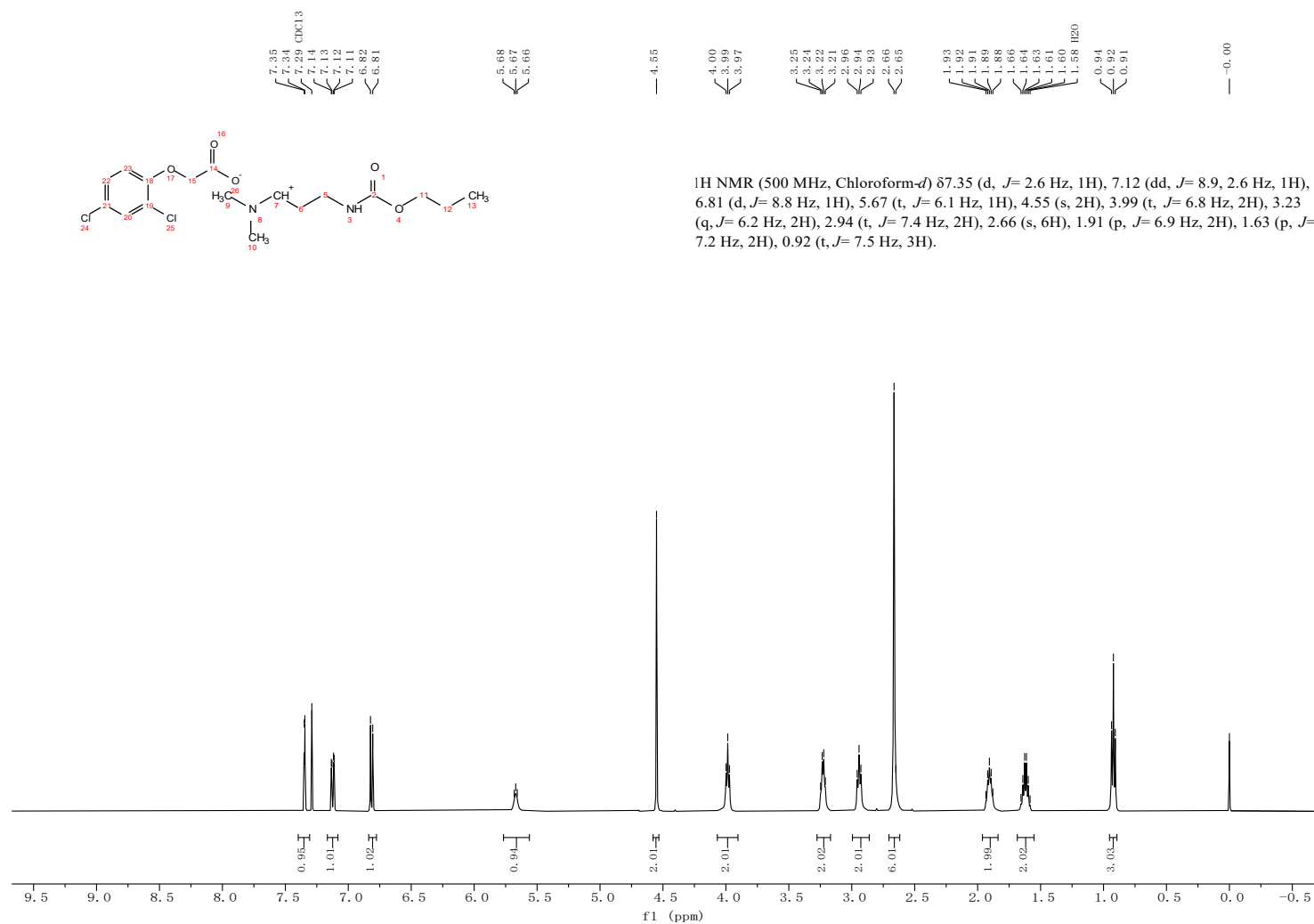


Fig. S11 ¹H NMR (500 MHz; CDCl₃; Me₄Si) of DIL-4 (2-(2,4-dichlorophenoxy)acetate N,N-dimethyl-3-((propoxycarbonyl)amino)propan-1-ylum-1-aminium)

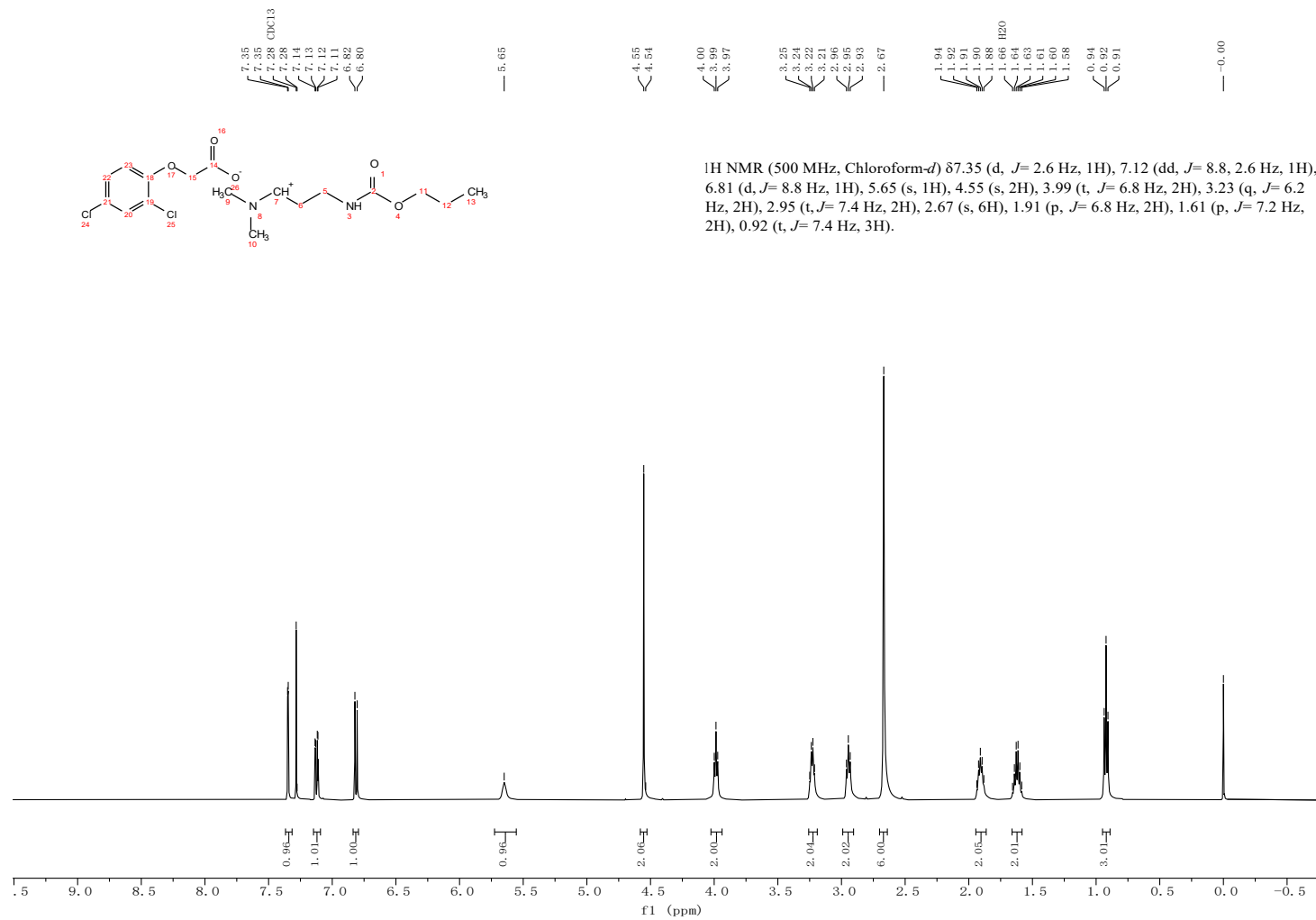


Fig. S12 ¹H NMR (500 MHz; CDCl₃; Me₄Si) of DIL-4 after volatility test

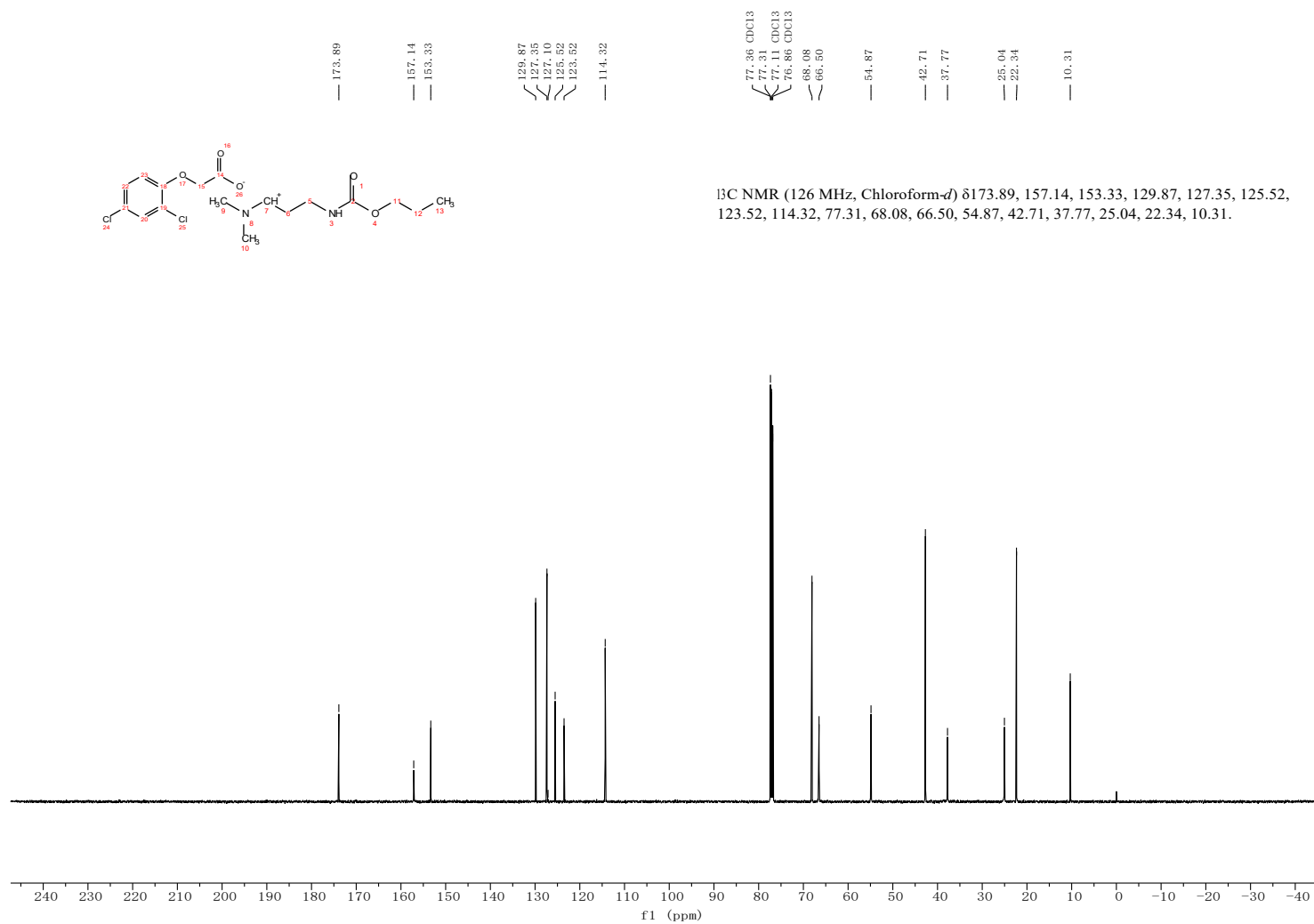


Fig. S13 ¹³C NMR (126 MHz; CDCl₃; Me₄Si) of DIL-4 (2-(2,4-dichlorophenoxy)acetate N,N-dimethyl-3-((propoxycarbonyl)amino)propan-1-ylum-1-aminium)

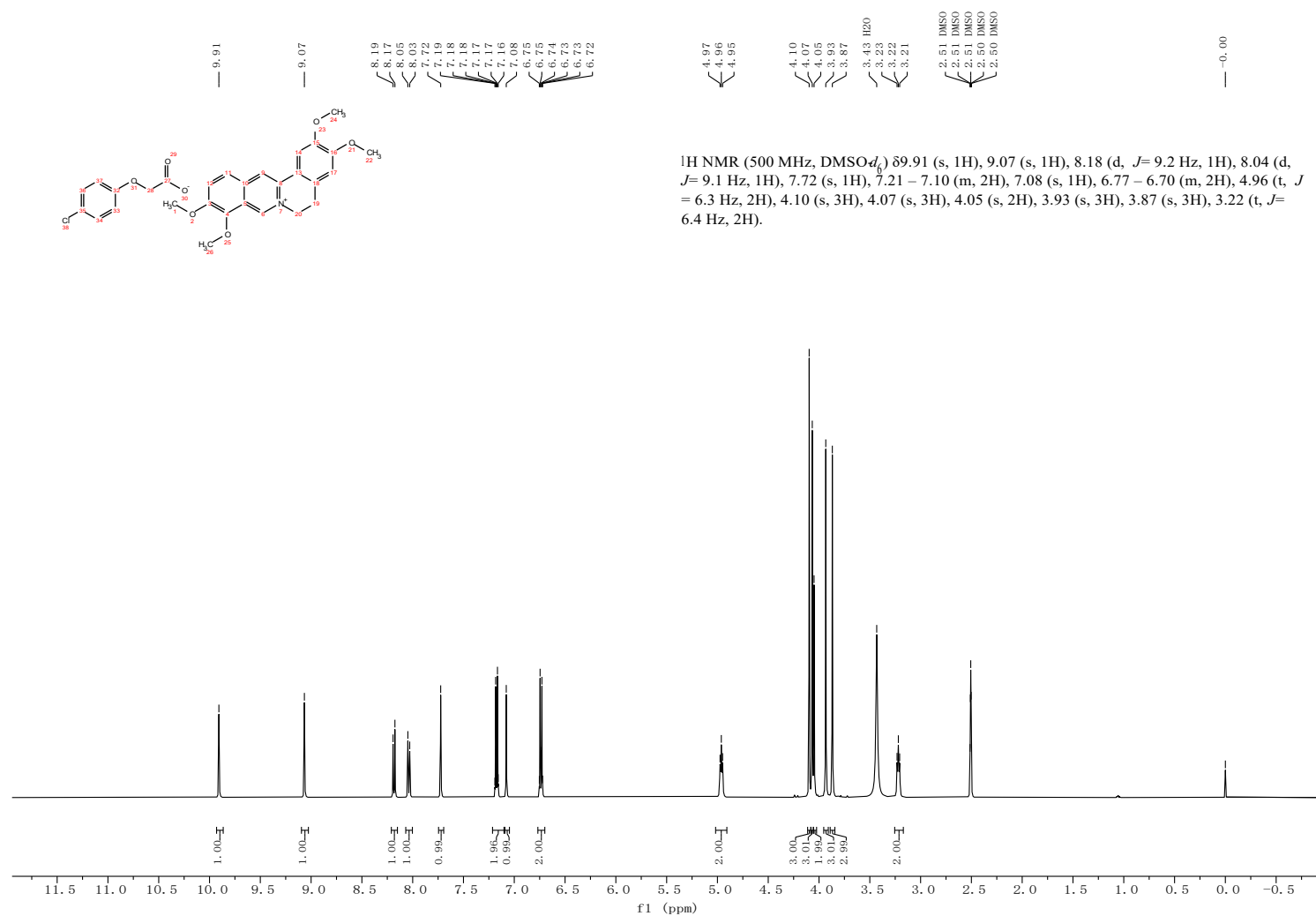
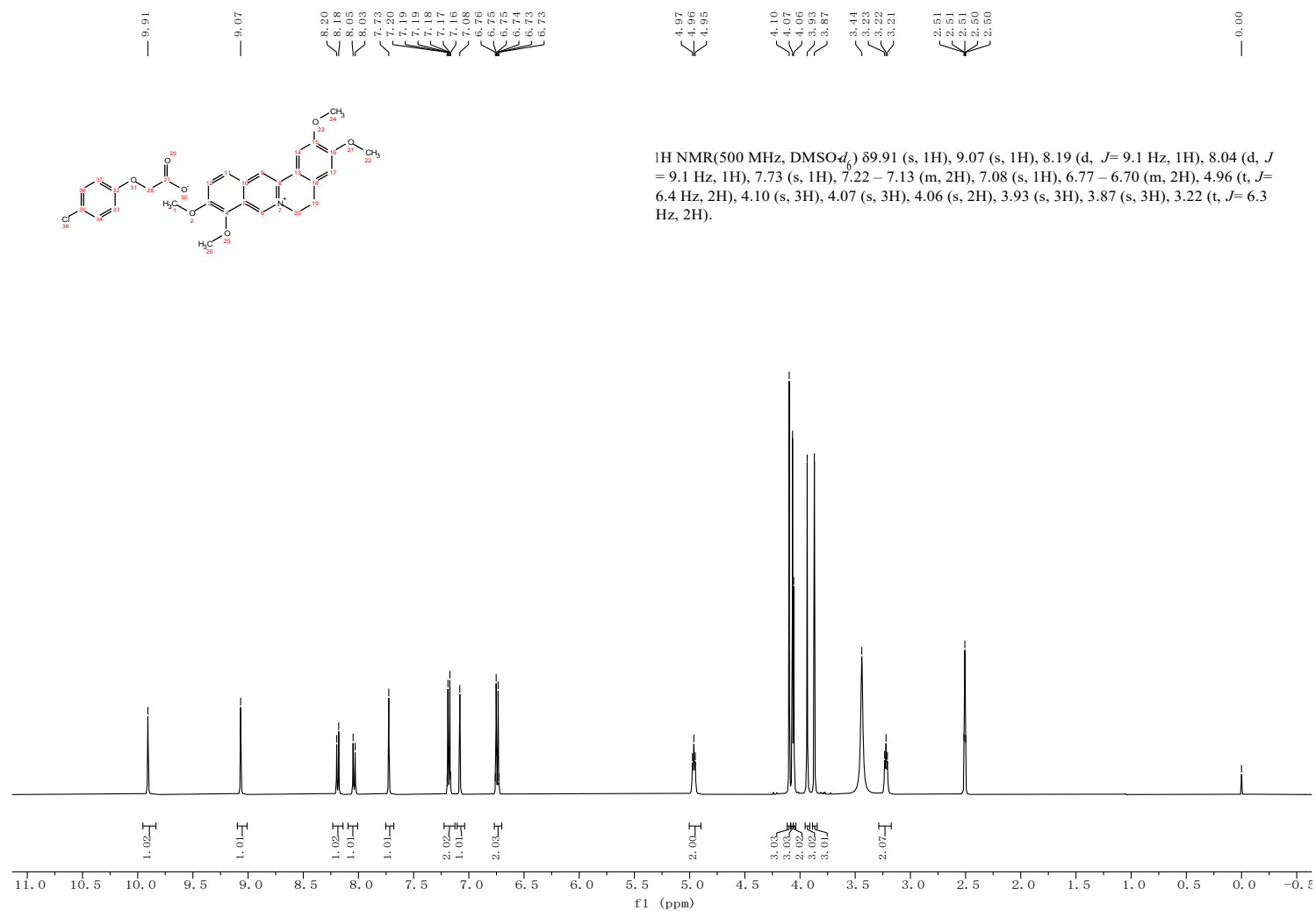


Fig. S14 ¹H NMR (500 MHz; DMSO-*d*₆; Me₄Si) of CIL-1 (2-(4-chlorophenoxy)acetate 2,3,9,10-tetramethoxy-5,6-dihydroisoquinolino[3,2-*a*]isoquinolin-7-ium)



¹H NMR(500 MHz, DMSO-*d*₆) δ9.91 (s, 1H), 9.07 (s, 1H), 8.19 (d, *J* = 9.1 Hz, 1H), 8.04 (d, *J* = 9.1 Hz, 1H), 7.73 (s, 1H), 7.22 – 7.13 (m, 2H), 7.08 (s, 1H), 6.77 – 6.70 (m, 2H), 4.96 (t, *J* = 6.4 Hz, 2H), 4.10 (s, 3H), 4.07 (s, 3H), 4.06 (s, 2H), 3.93 (s, 3H), 3.87 (s, 3H), 3.22 (t, *J* = 6.3 Hz, 2H).

Fig. S15 ¹H NMR (500 MHz; DMSO-*d*₆; Me₄Si) of CIL-1 after volatility test

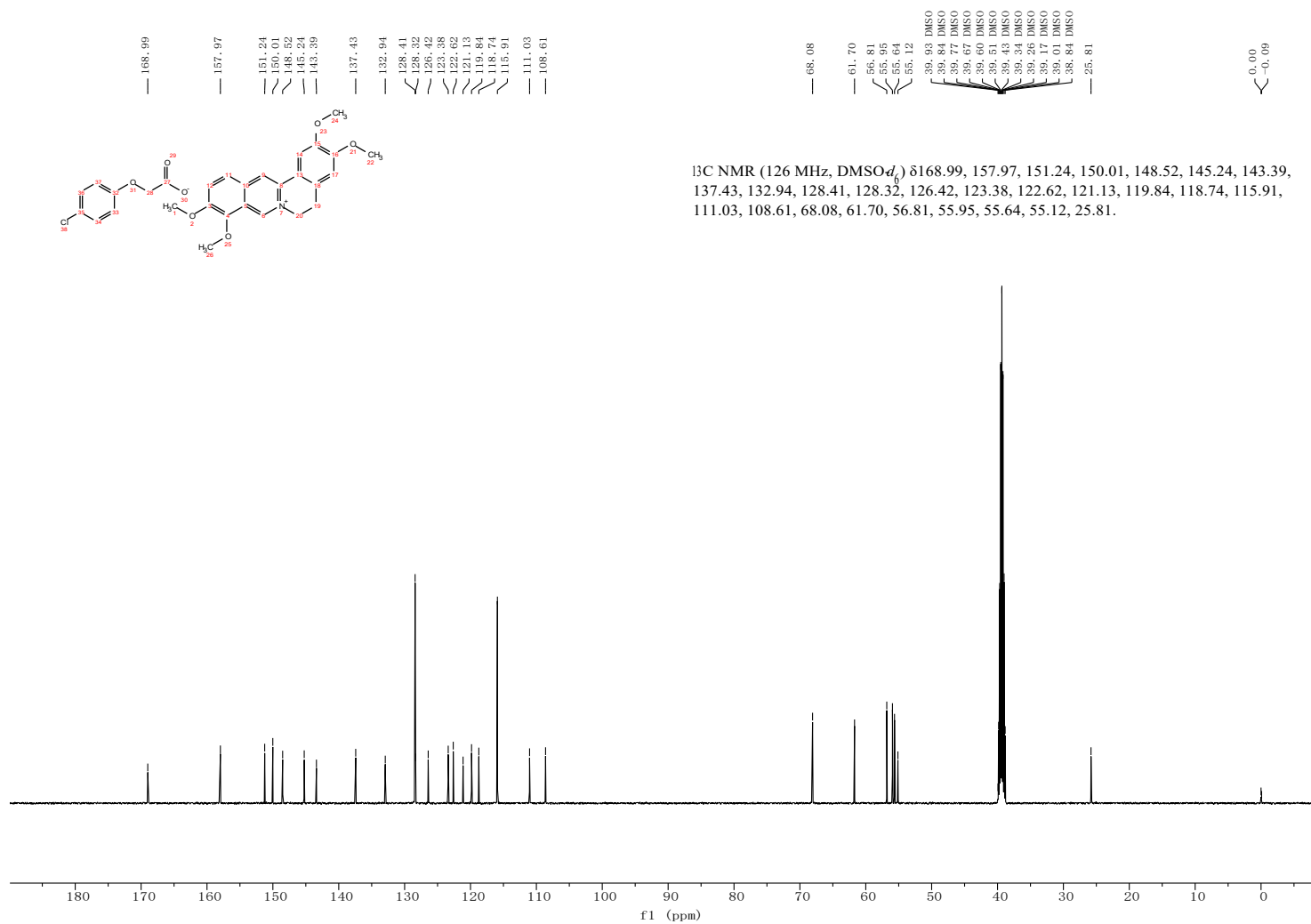


Fig. S16 ^{13}C NMR (126 MHz; $\text{DMSO-}d_6$; Me_4Si) of CIL-1 (2-(4-chlorophenoxy)acetate 2,3,9,10-tetramethoxy-5,6-dihydroisoquinolino[3,2-a]isoquinolin-7-ium)

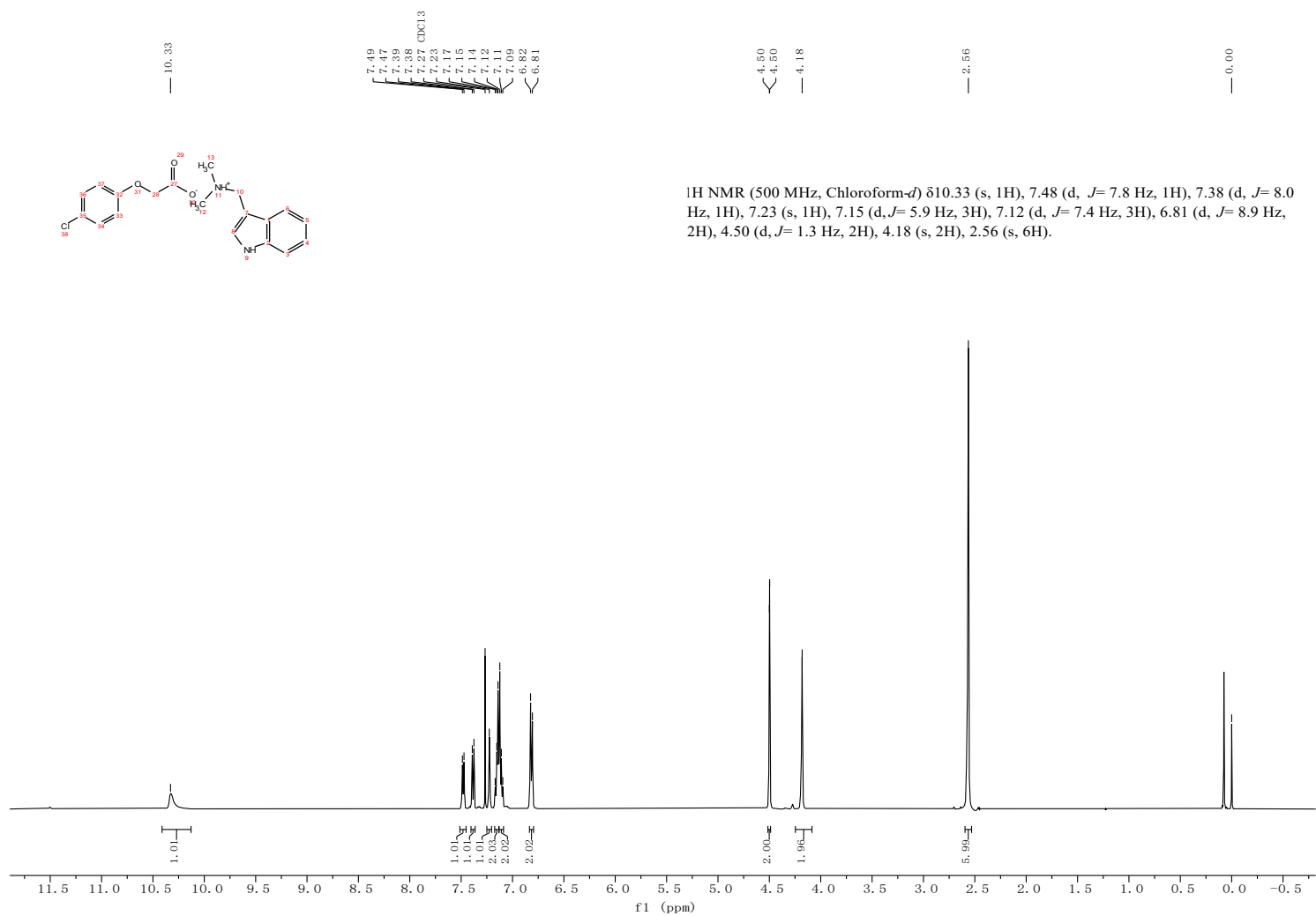


Fig. S17 ¹H NMR (500 MHz; CDCl₃; Me₄Si) of CIL-2 (2-(4-chlorophenoxy)acetate 1-(1H-indol-3-yl)-N,N-dimethylmethanaminium)

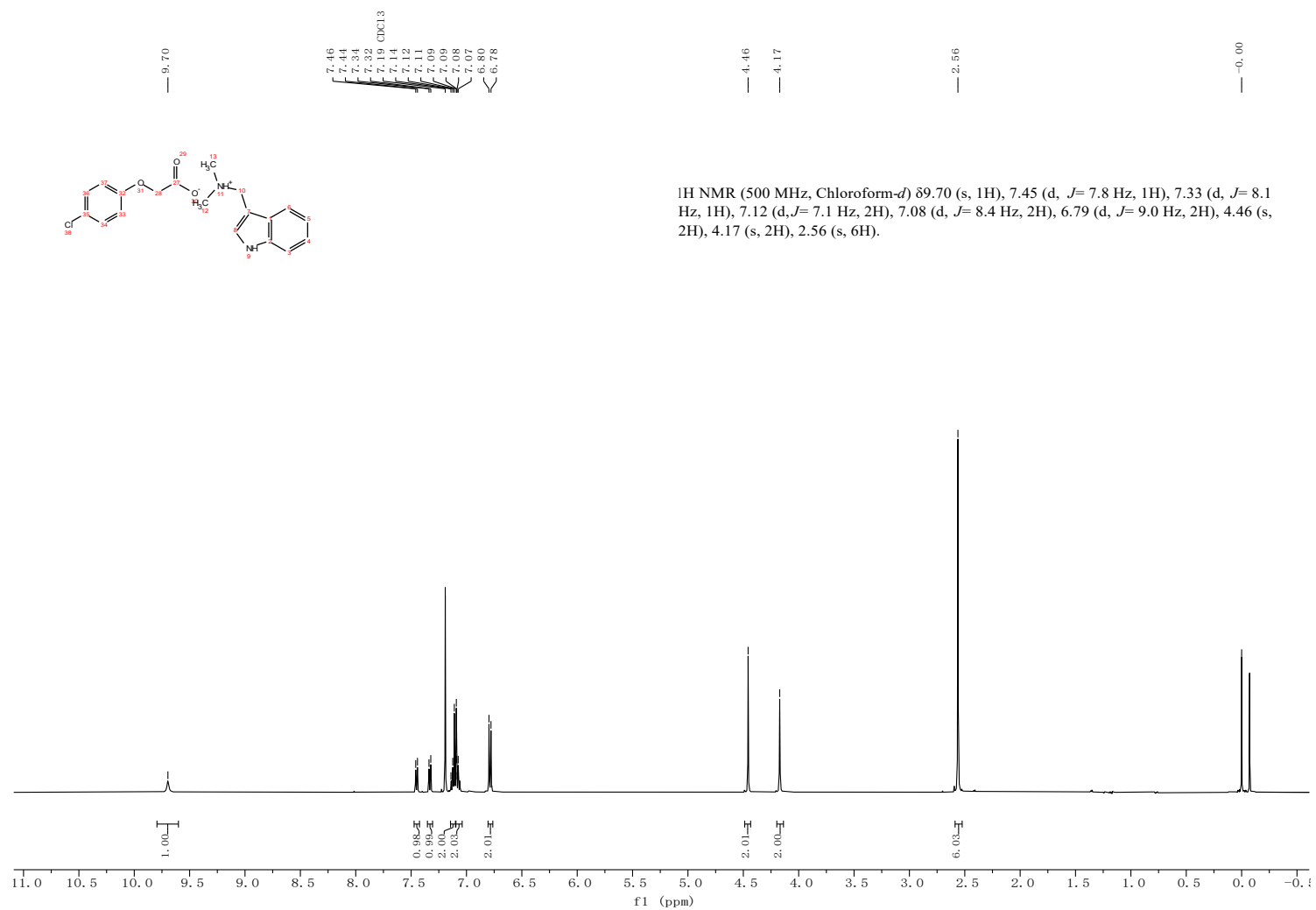


Fig. S18 ¹H NMR (500 MHz; CDCl₃; Me₄Si) of CIL-2 after volatility test

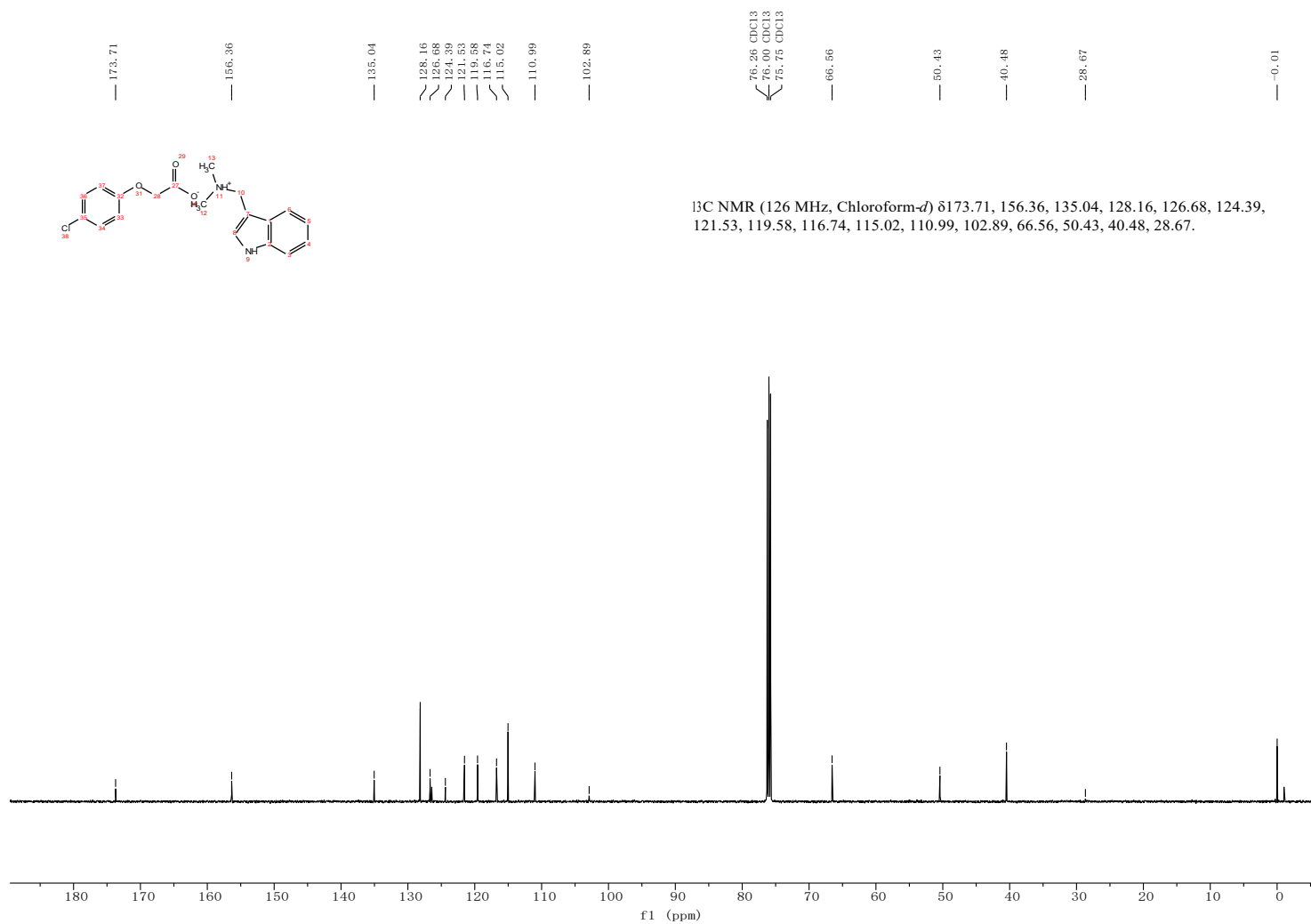


Fig. S19 ^{13}C NMR (126 MHz; CDCl_3 ; Me_4Si) of CIL-2 (2-(4-chlorophenoxy)acetate 1-(1H-indol-3-yl)-N,N-dimethylmethanaminium)

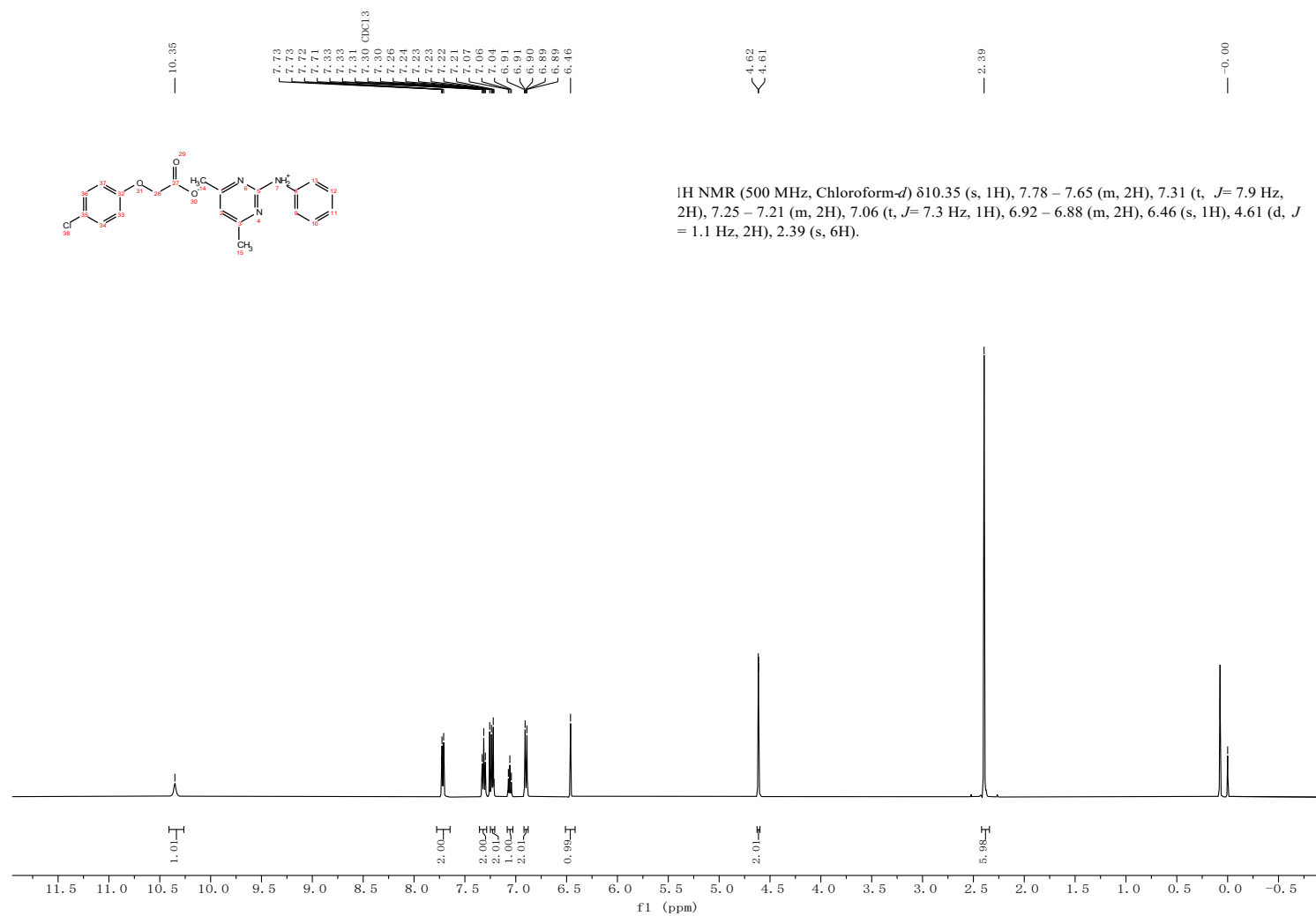


Fig. S20 ¹H NMR (500 MHz; CDCl₃; Me₄Si) of CIL-3 (2-(4-chlorophenoxy)acetate 4,6-dimethyl-N-phenylpyrimidin-2-aminium)

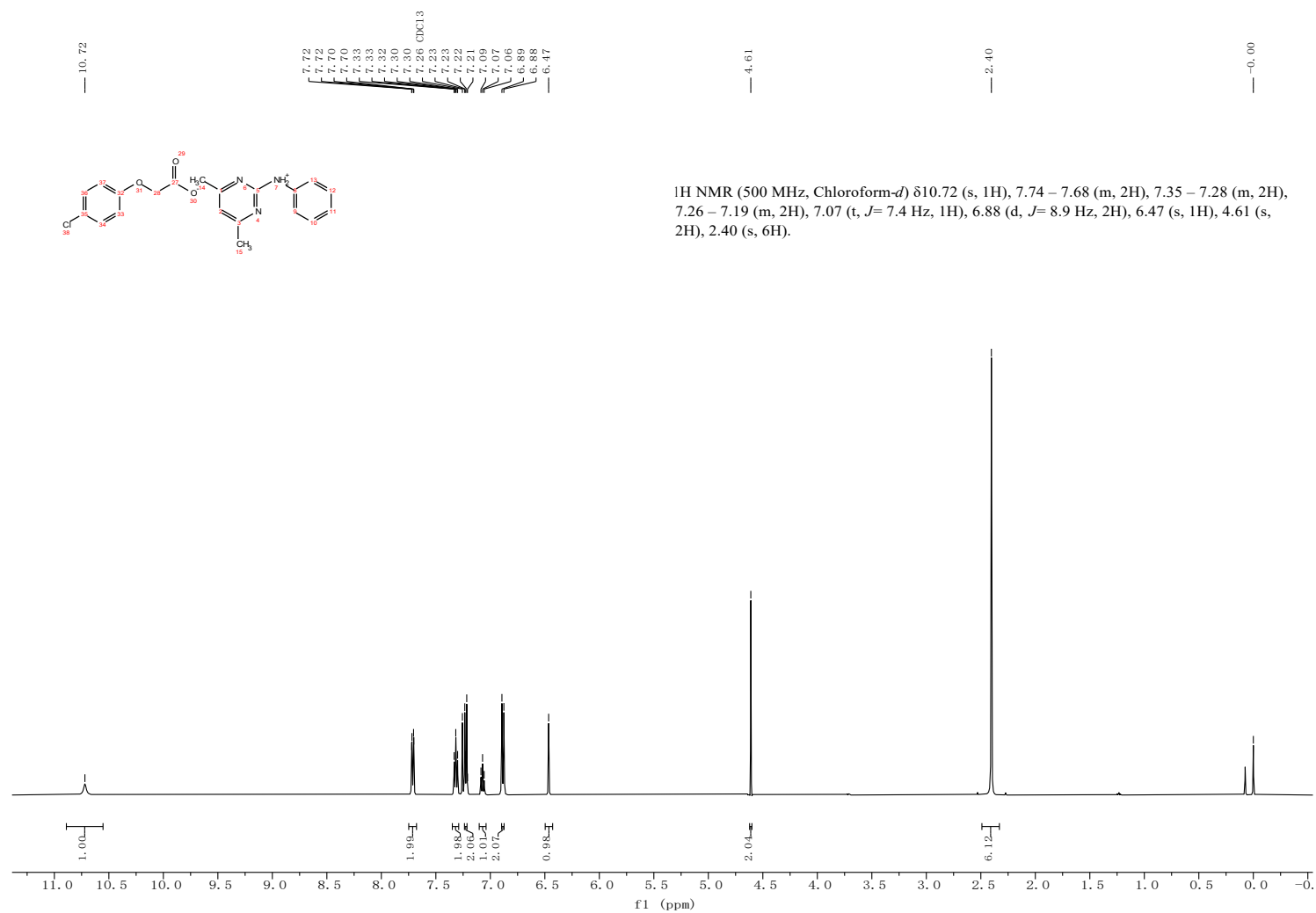


Fig. S21 ¹H NMR (500 MHz; CDCl₃; Me₄Si) of CIL-3 after volatility test

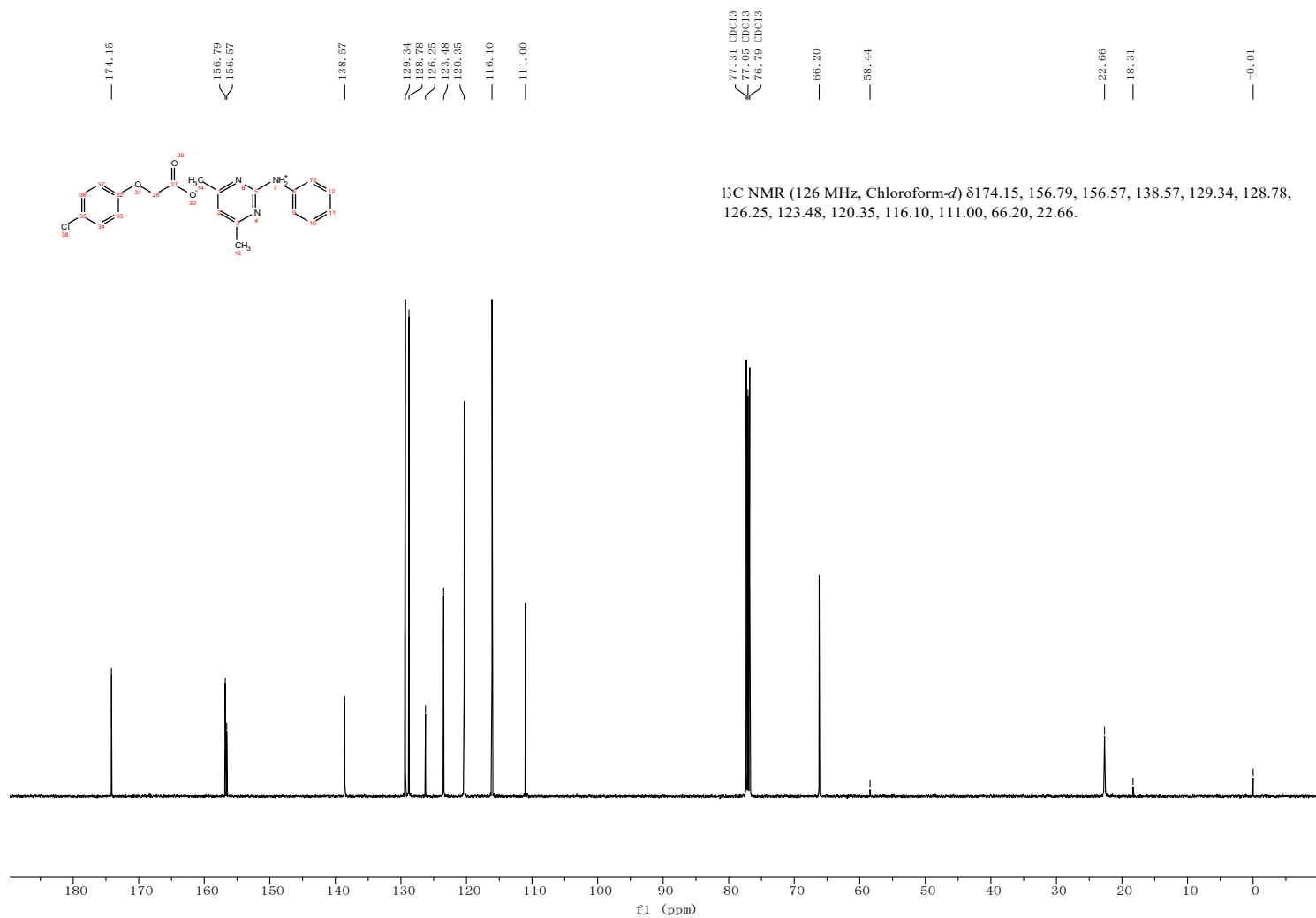


Fig. S22 ^{13}C NMR (126 MHz; CDCl_3 ; Me_4Si) of CIL-3 (2-(4-chlorophenoxy)acetate 4,6-dimethyl-N-phenylpyrimidin-2-amium)

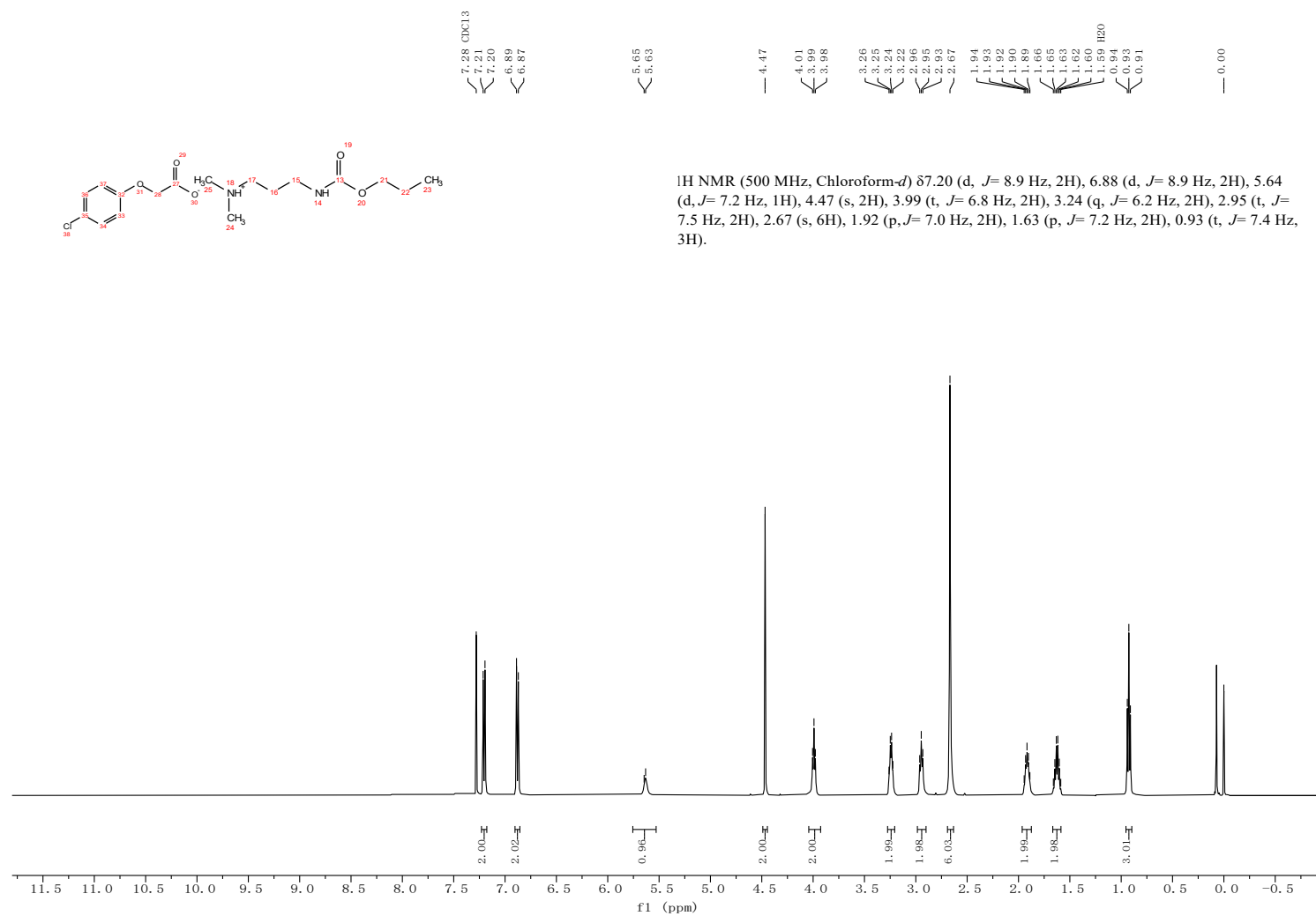


Fig. S23 ¹H NMR (500 MHz; CDCl₃; Me₄Si) of CIL-4 (2-(4-chlorophenoxy)acetate N,N-dimethyl-3-((propoxycarbonyl)amino)propan-1-ylum-1-aminium)

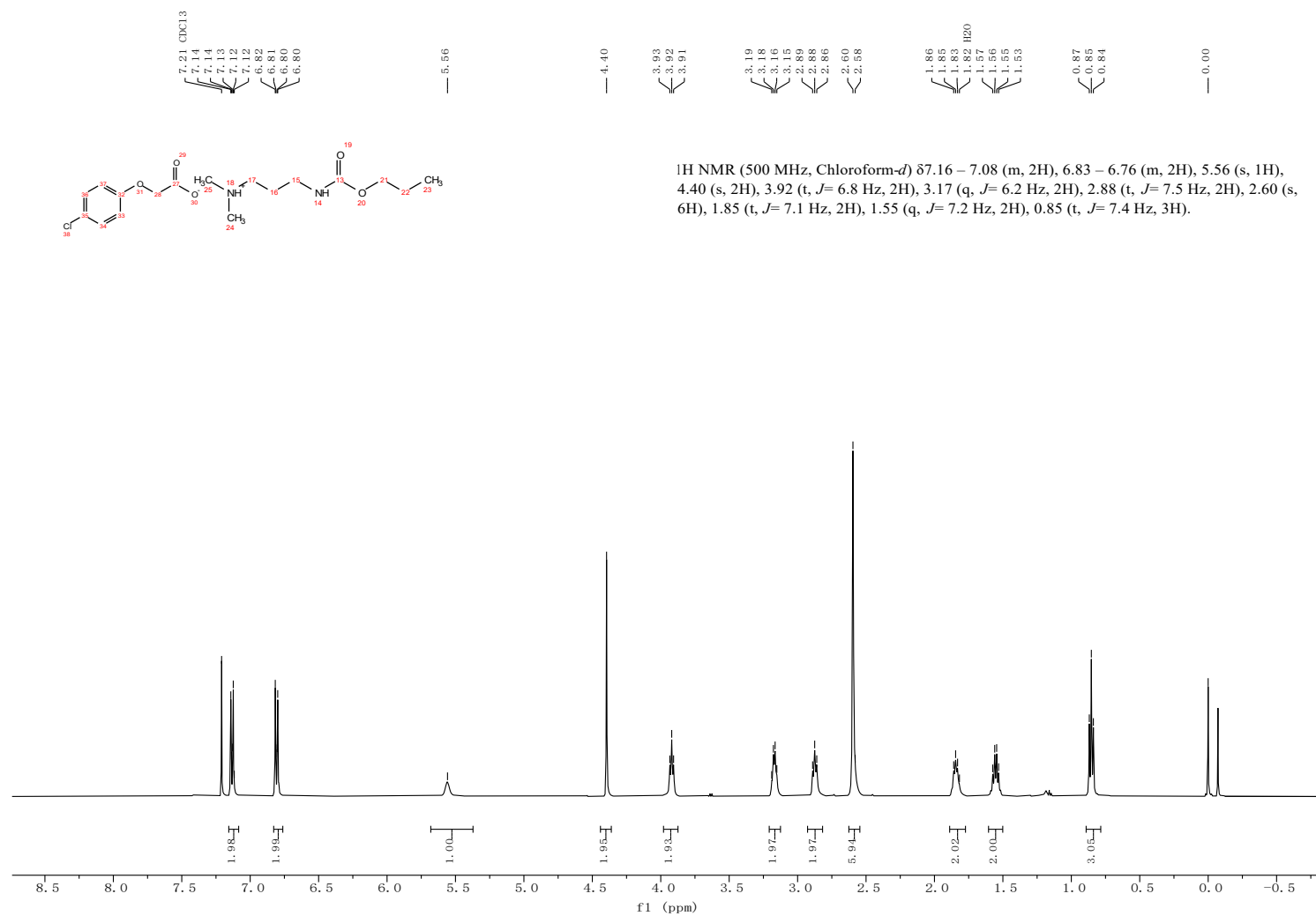


Fig. S24 ¹H NMR (500 MHz; CDCl₃; Me₄Si) of CIL-4 after volatility test

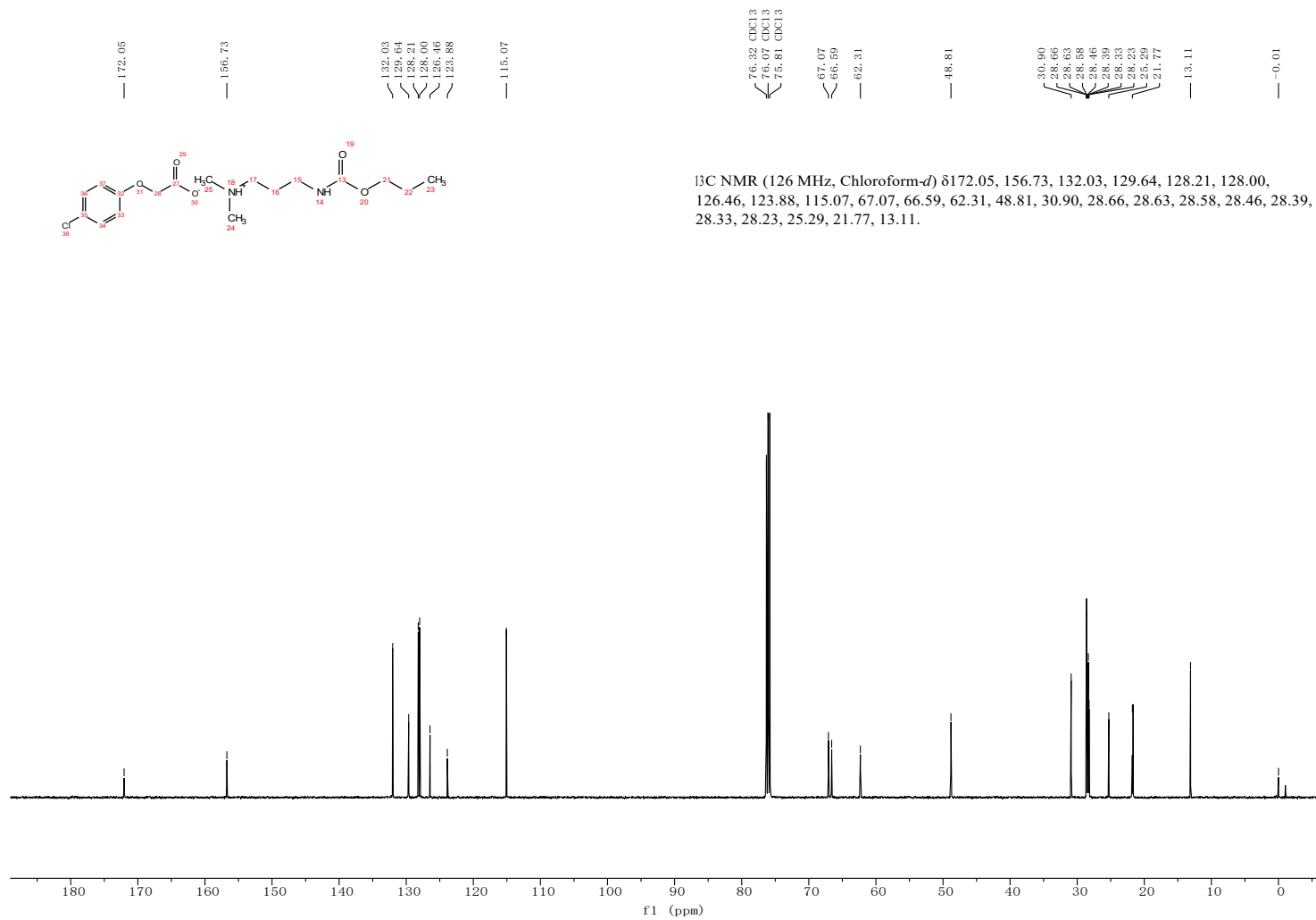


Fig. S25 ¹³C NMR (126 MHz; CDCl₃; Me₄Si) of CIL-4 (2-(4-chlorophenoxy)acetate N,N-dimethyl-3-((propoxycarbonyl)amino)propan-1-ylum-1-aminium)

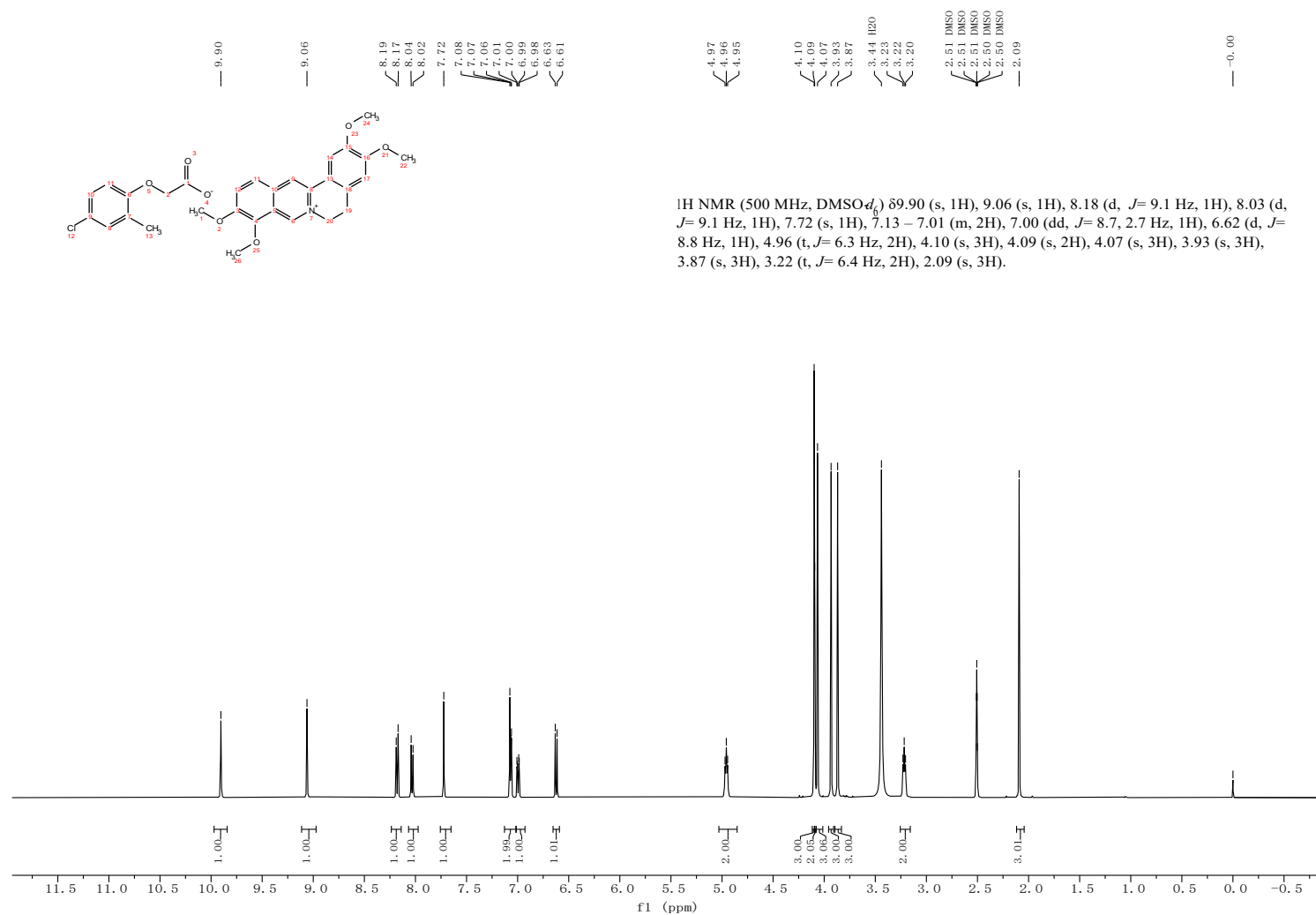


Fig. S26 ¹H NMR (500 MHz; DMSO-*d*₆; Me₄Si) of MIL-1 (2-(4-chloro-2-methylphenoxy)acetate 2,3,9,10-tetramethoxy-5,6-dihydroisoquinolino[3,2-a]isoquinolin-7-ium)

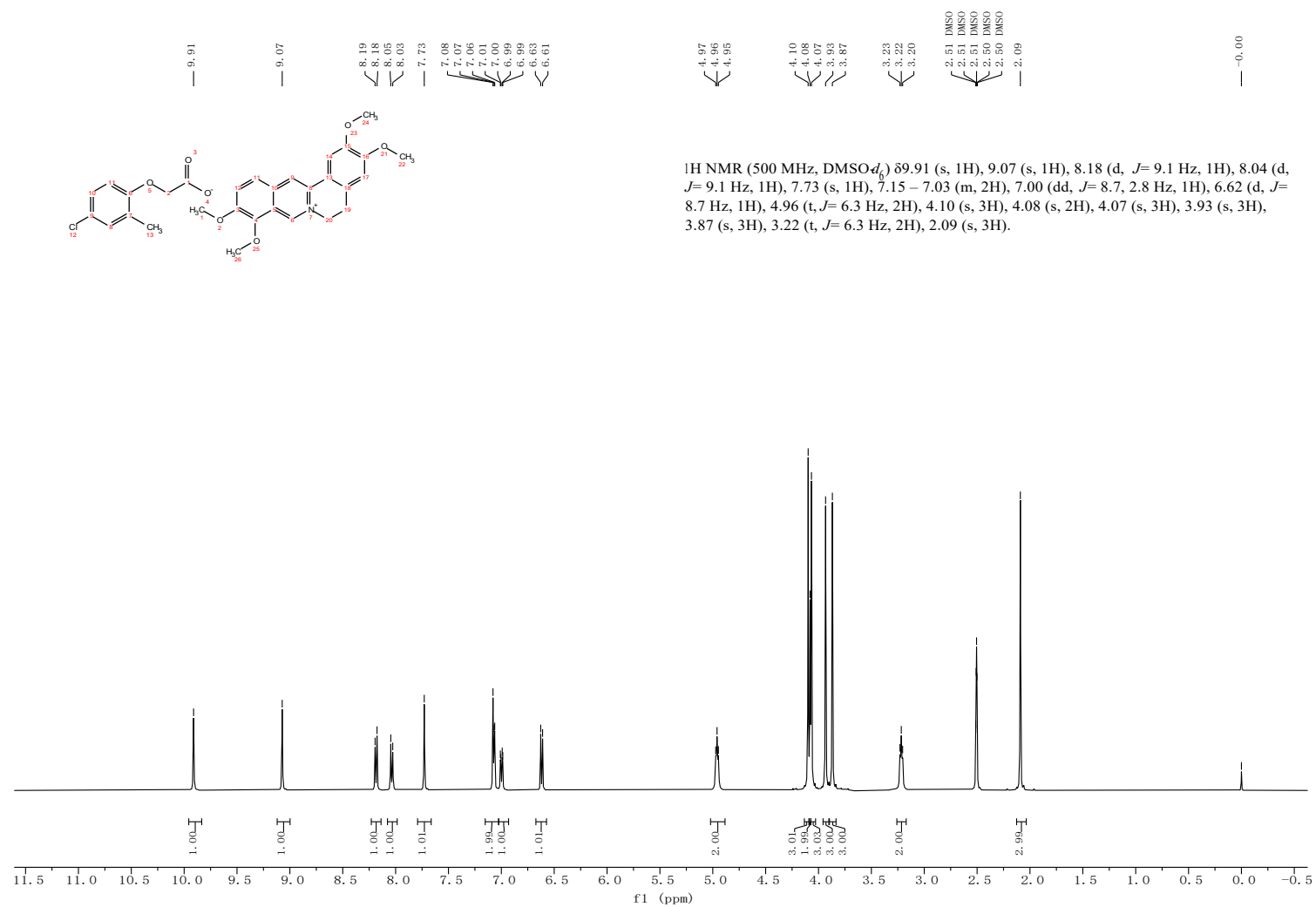


Fig. S27 $^1\text{H NMR}$ (500 MHz; DMSO-d_6 ; Me_4Si) of MIL-1 after volatility test

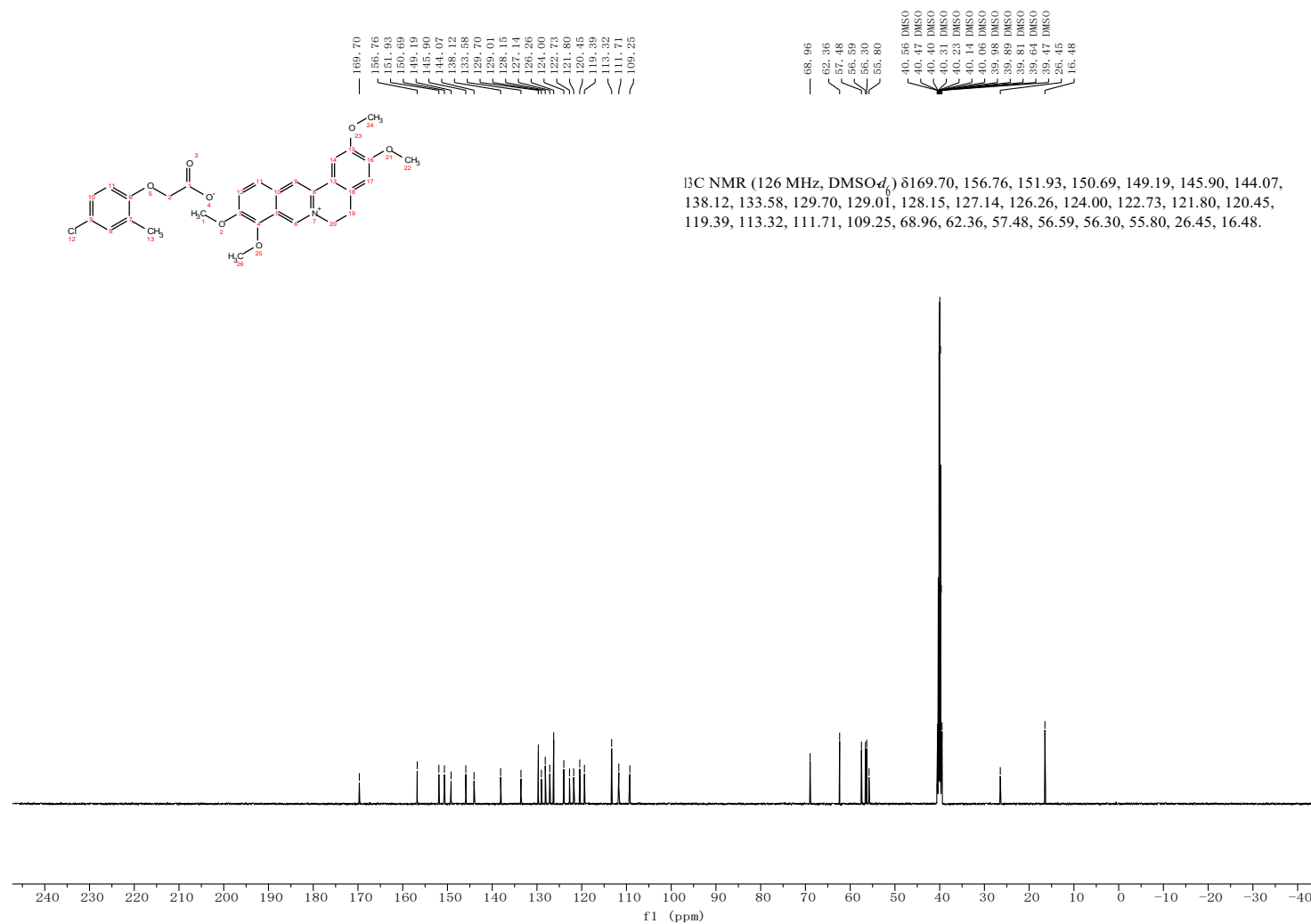


Fig. S28 ^{13}C NMR (126 MHz; $\text{DMSO-}d_6$; Me_4Si) of MIL-1 (2-(4-chloro-2-methylphenoxy)acetate 2,3,9,10-tetramethoxy-5,6-dihydroisoquinolino[3,2-a]isoquinolin-7-ium)

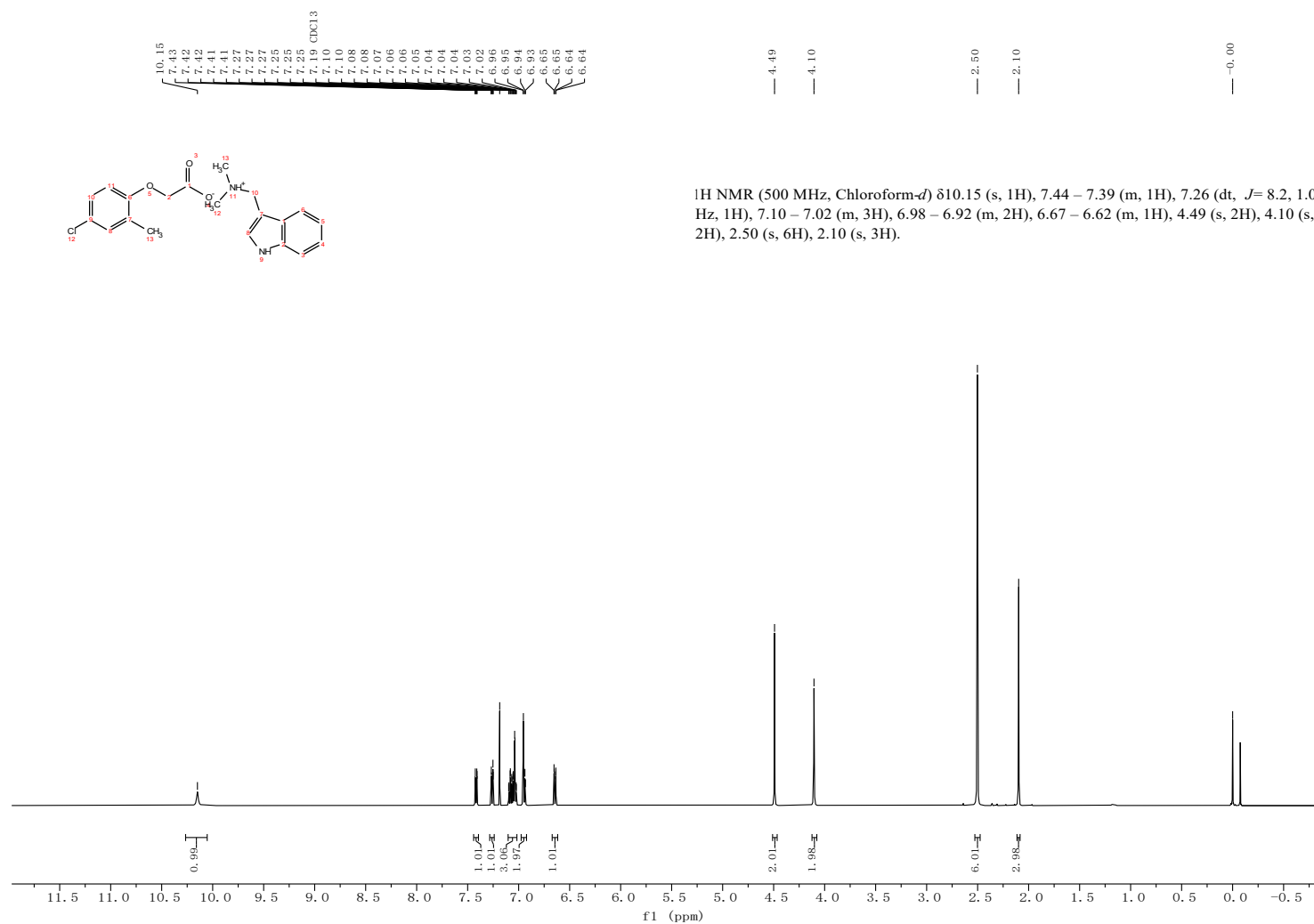
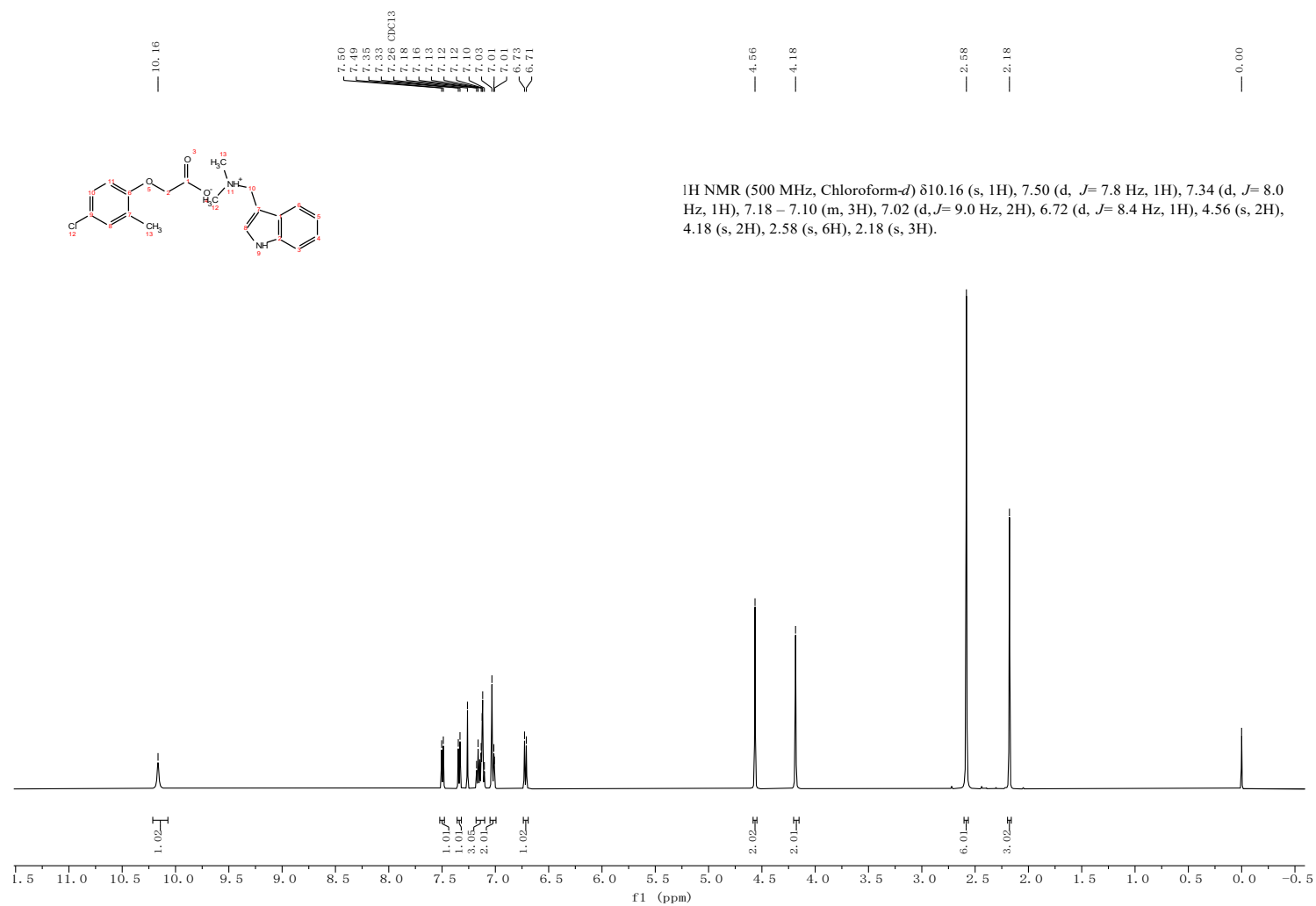


Fig. S29 ^1H NMR (500 MHz; CDCl_3 ; Me $_4\text{Si}$) of MIL-2 (2-(4-chloro-2-methylphenoxy)acetate 1-(1H-indol-3-yl)-N,N-dimethylmethanaminium)



^1H NMR (500 MHz, Chloroform-*d*) δ 10.16 (s, 1H), 7.50 (d, $J=7.8$ Hz, 1H), 7.34 (d, $J=8.0$ Hz, 1H), 7.18 – 7.10 (m, 3H), 7.02 (d, $J=9.0$ Hz, 2H), 6.72 (d, $J=8.4$ Hz, 1H), 4.56 (s, 2H), 4.18 (s, 2H), 2.58 (s, 6H), 2.18 (s, 3H).

Fig. S30 ^1H NMR (500 MHz; CDCl_3 ; Me_4Si) of MIL-2 after volatility test

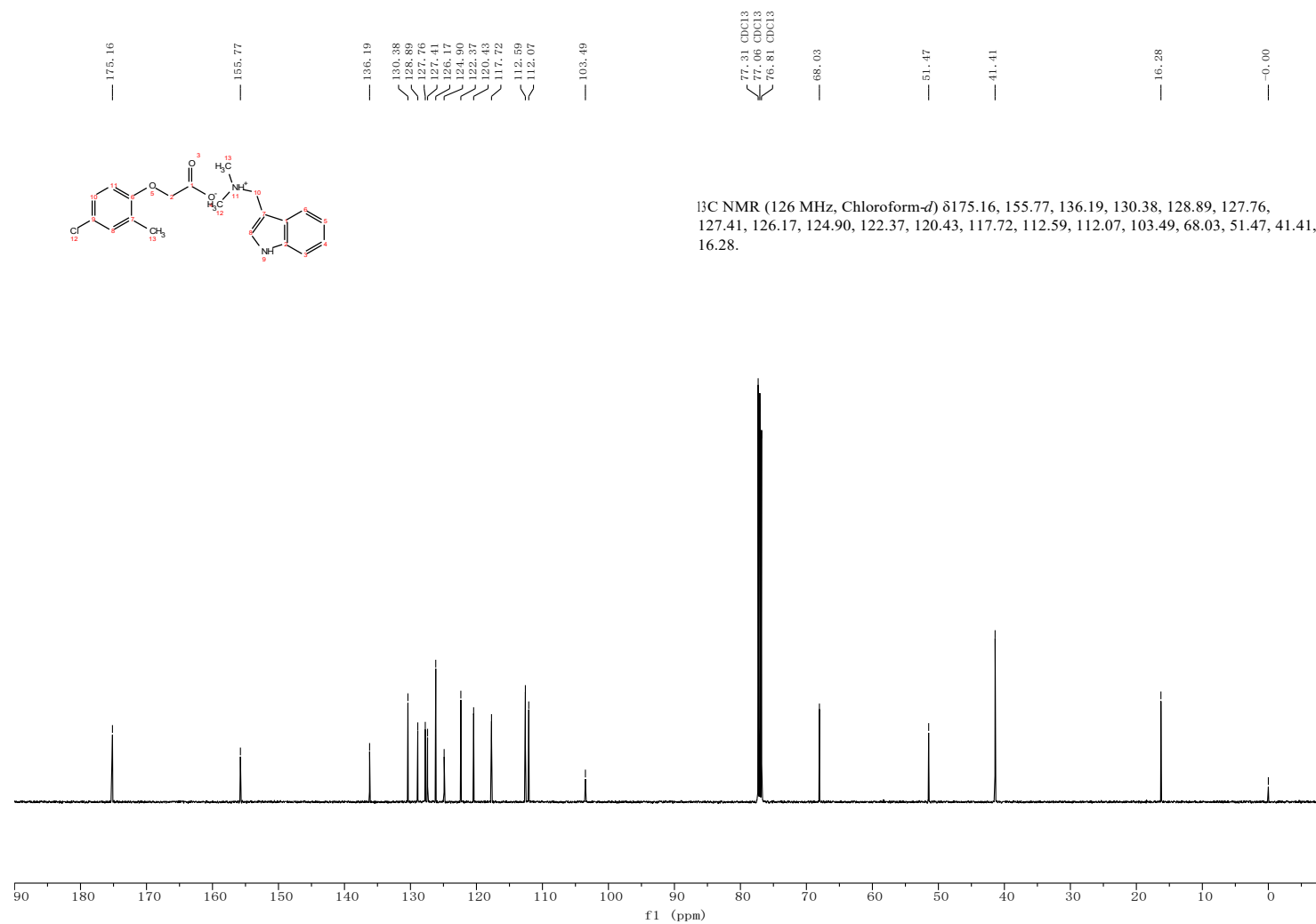


Fig. S31 ¹³C NMR (126 MHz; CDCl₃; Me₄Si) of MIL-2 (2-(4-chloro-2-methylphenoxy)acetate 1-(1H-indol-3-yl)-N,N-dimethylmethanaminium)

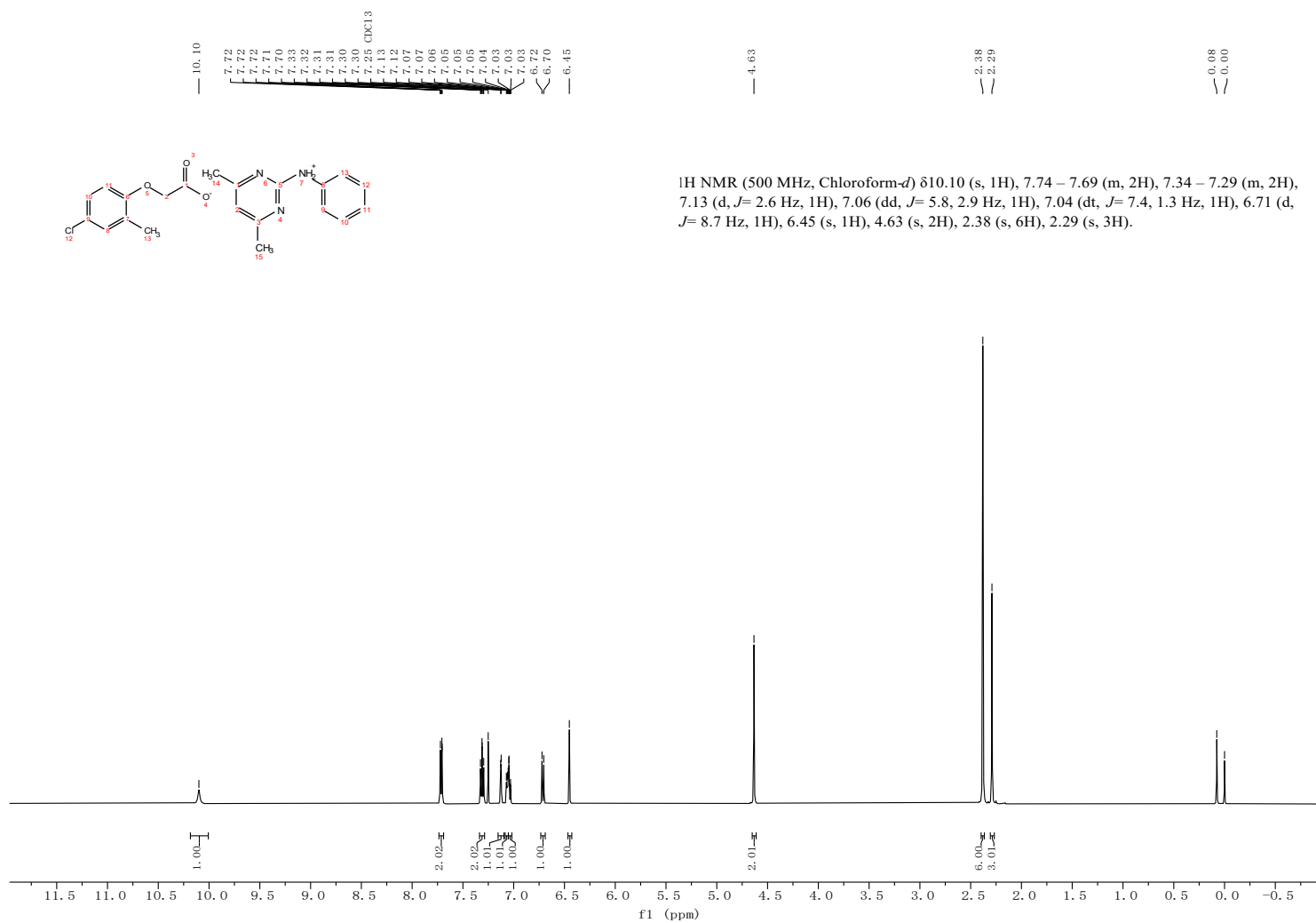


Fig. S32 ¹H NMR (500 MHz; CDCl₃; Me₄Si) of MIL-3 (2-(4-chlorophenoxy)acetate 4,6-dimethyl-N-phenylpyrimidin-2-aminium)

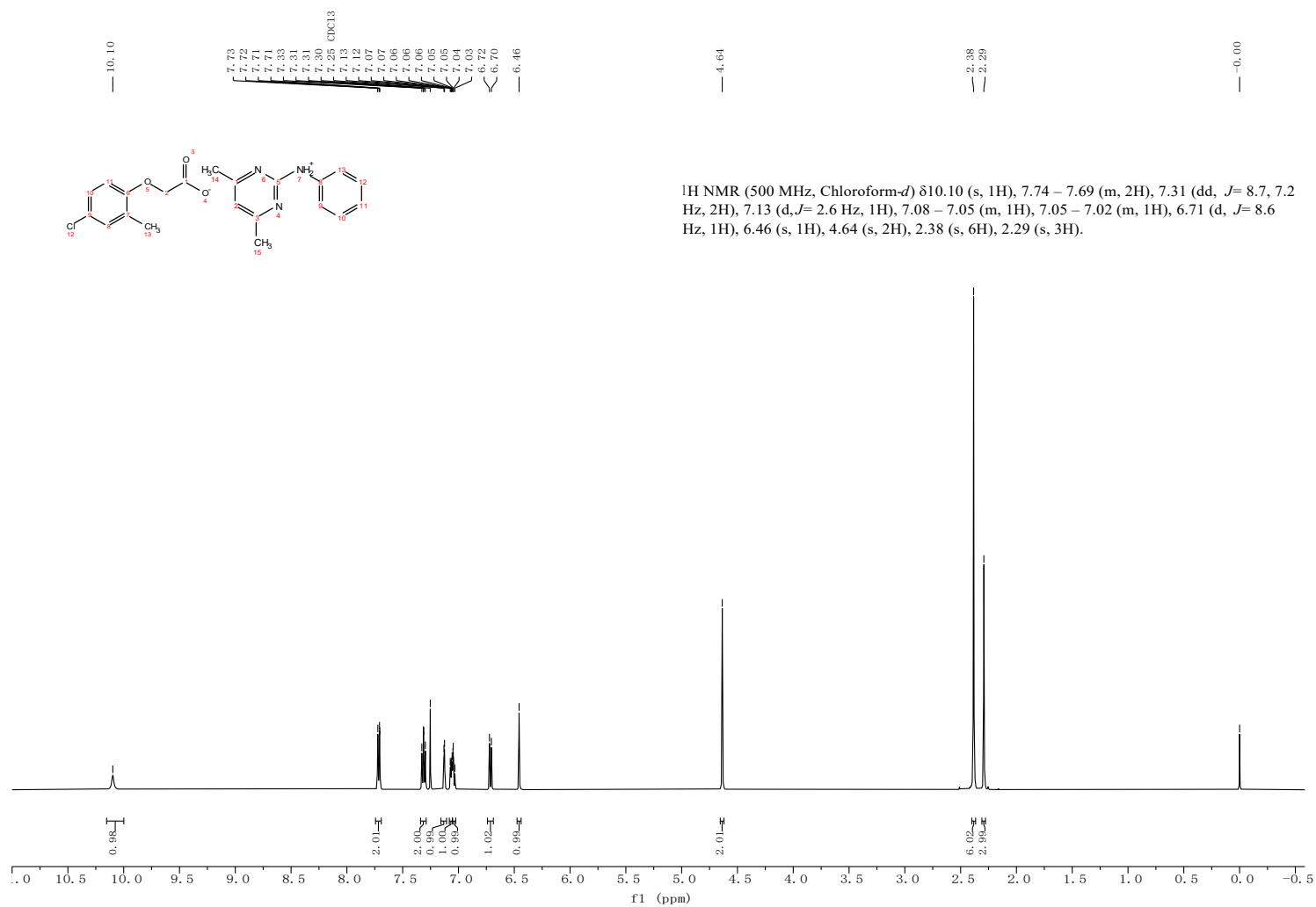


Fig. S33 ¹H NMR (500 MHz; CDCl₃; Me₄Si) of MIL-3 after volatility test

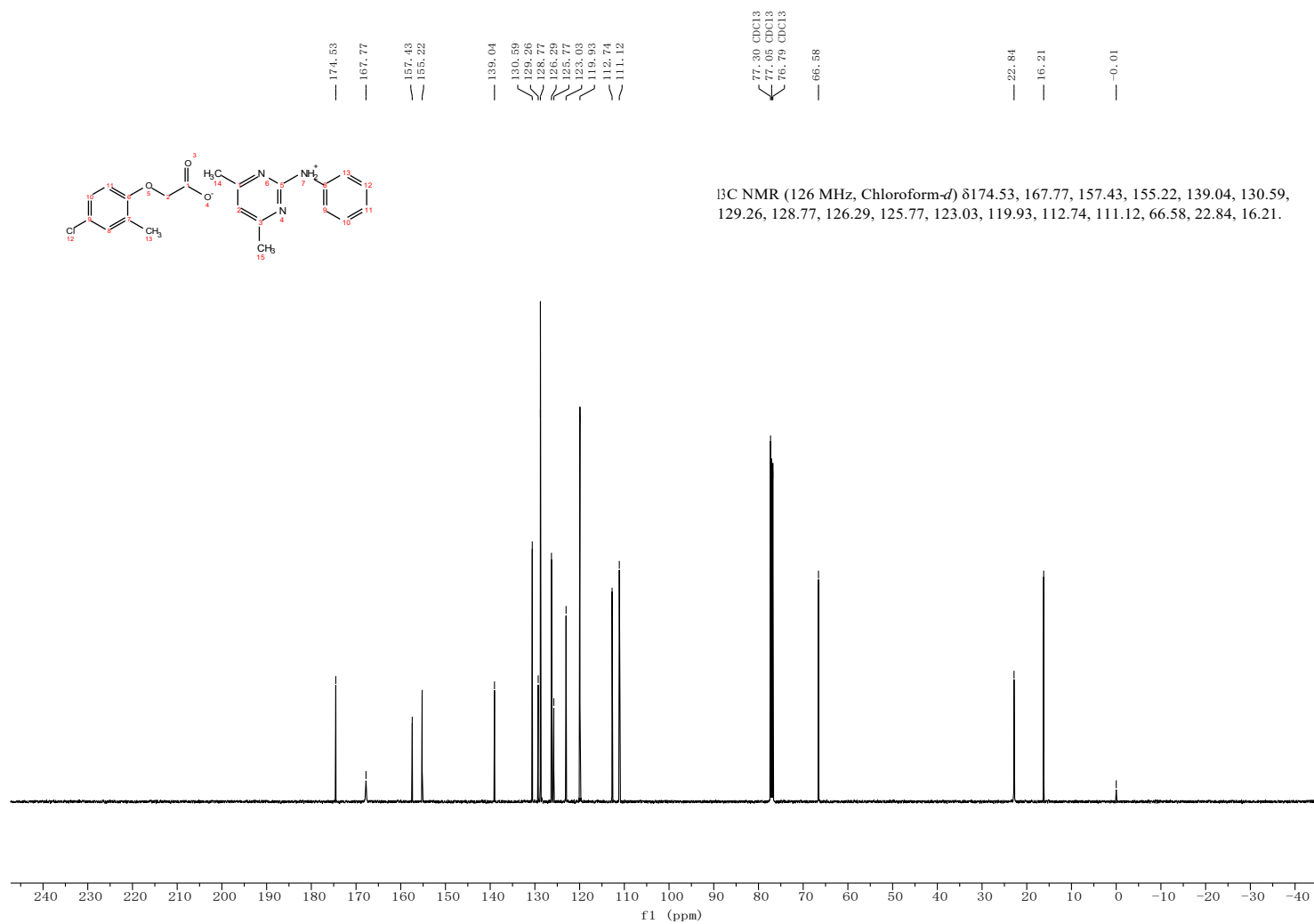


Fig. S34 ^{13}C NMR (126 MHz; CDCl_3 ; Me_4Si) of MIL-3 (2-(4-chlorophenoxy)acetate 4,6-dimethyl-N-phenylpyrimidin-2-aminium)

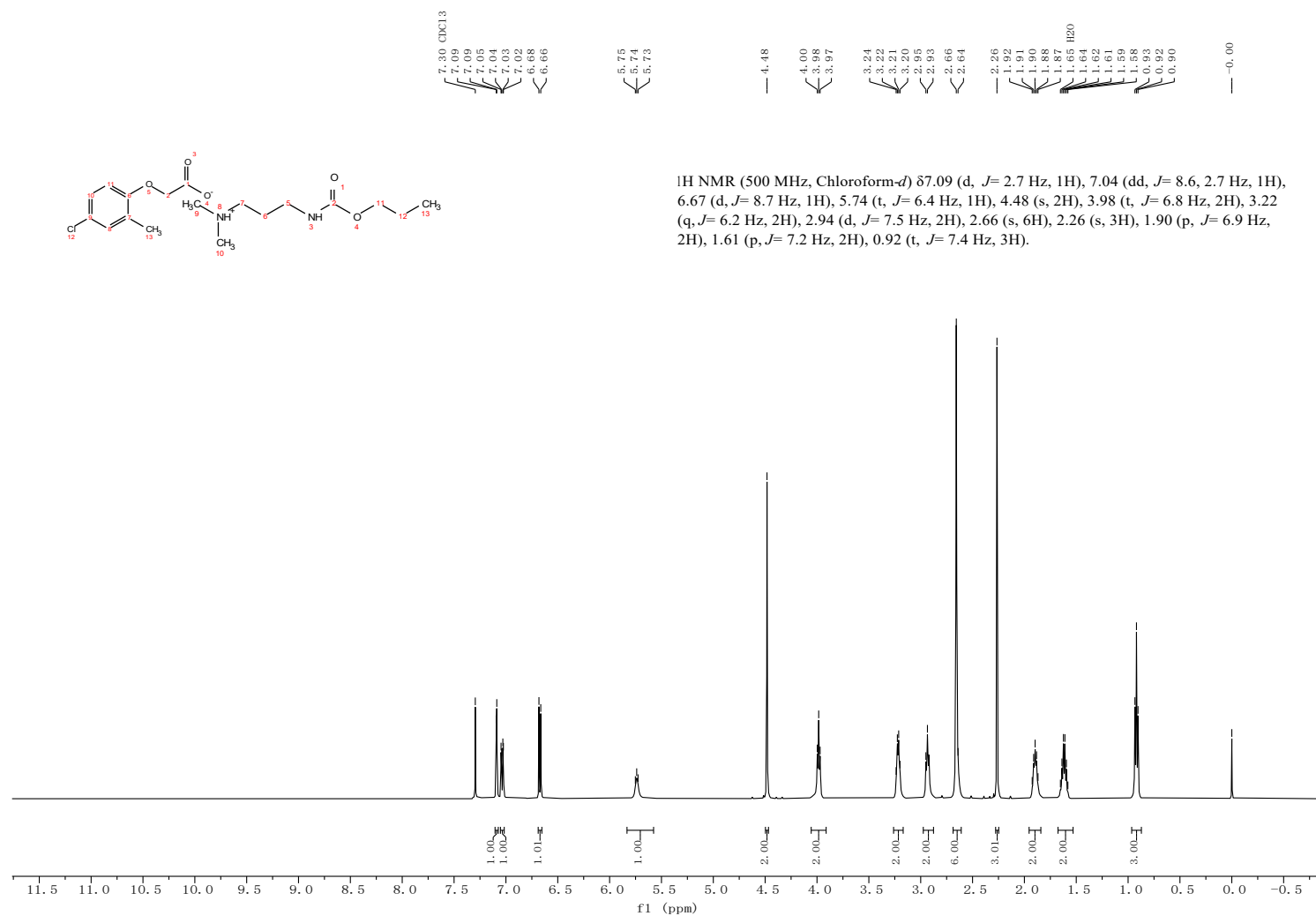


Fig. S35 ¹H NMR (500 MHz; CDCl₃; Me₄Si) of MIL-4 (2-(4-chloro-2-methylphenoxy)acetate N,N-dimethyl-3-((propoxycarbonyl)amino)propan-1-aminium)

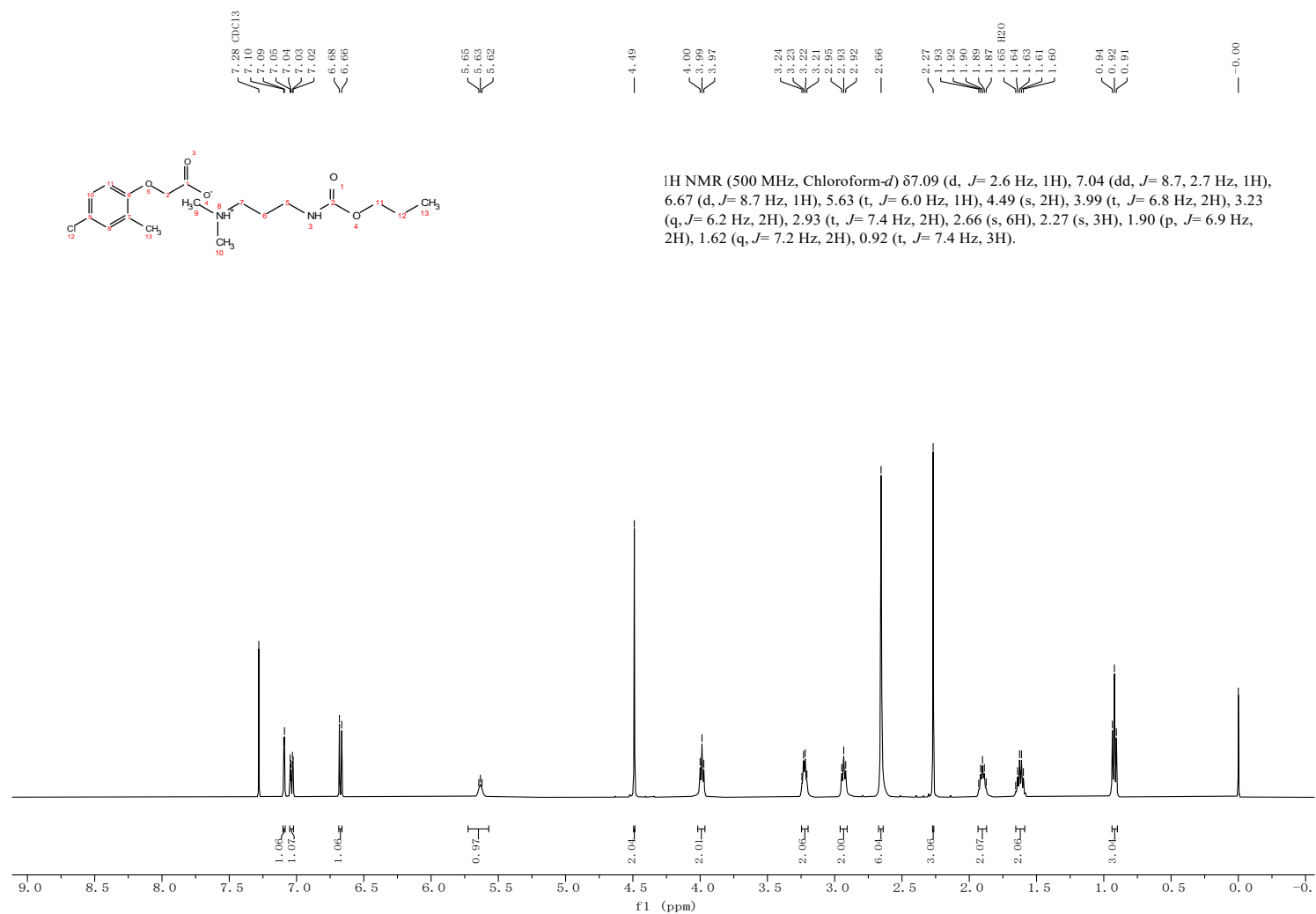


Fig. S36 ¹H NMR (500 MHz; CDCl₃; Me₄Si) of MIL-4 after volatility test

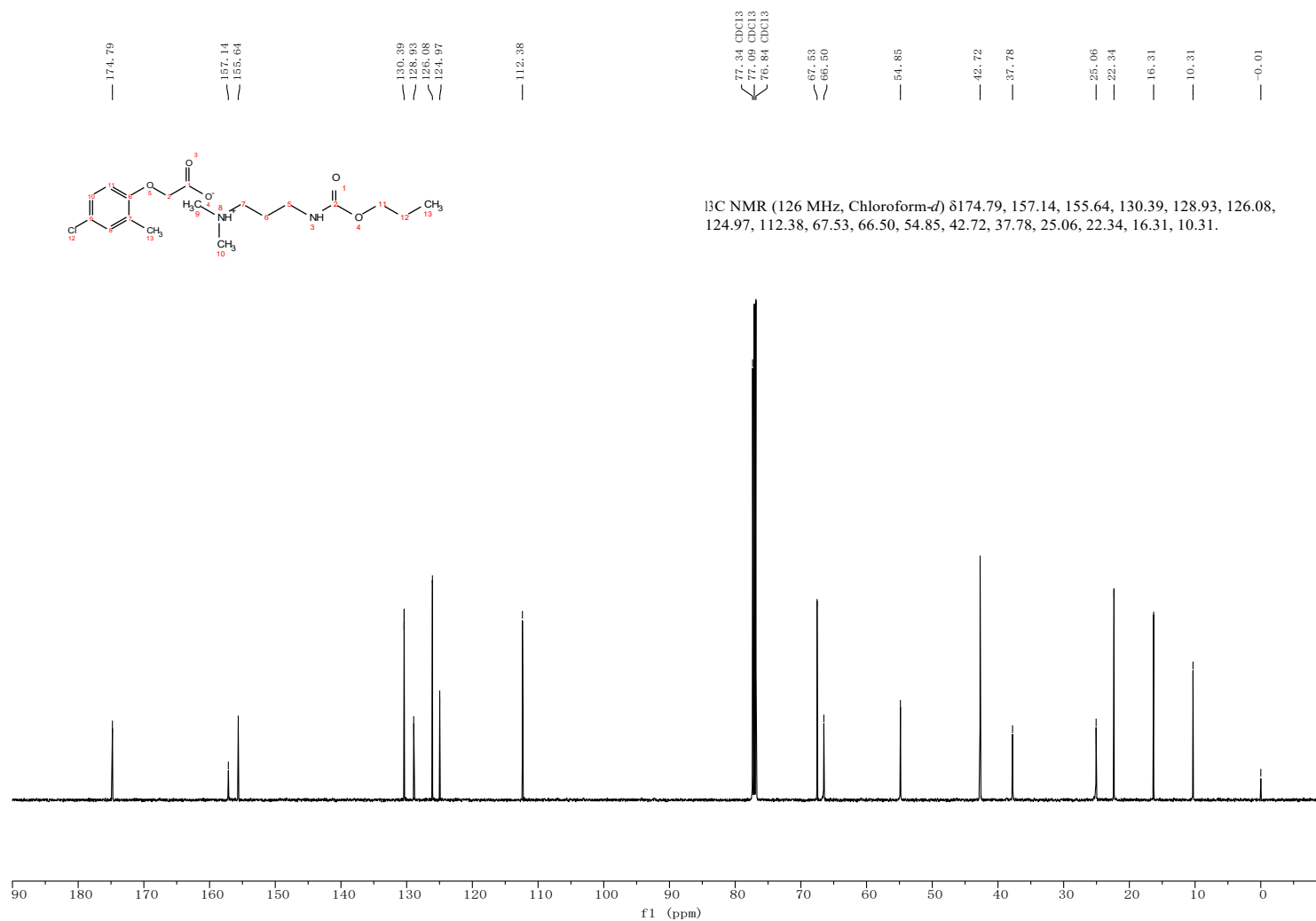


Fig. S37 ¹³C NMR (126 MHz; CDCl₃; Me₄Si) of MIL-4 (2-(4-chloro-2-methylphenoxy)acetate N,N-dimethyl-3-((propoxycarbonyl)amino)propan-1-aminium)

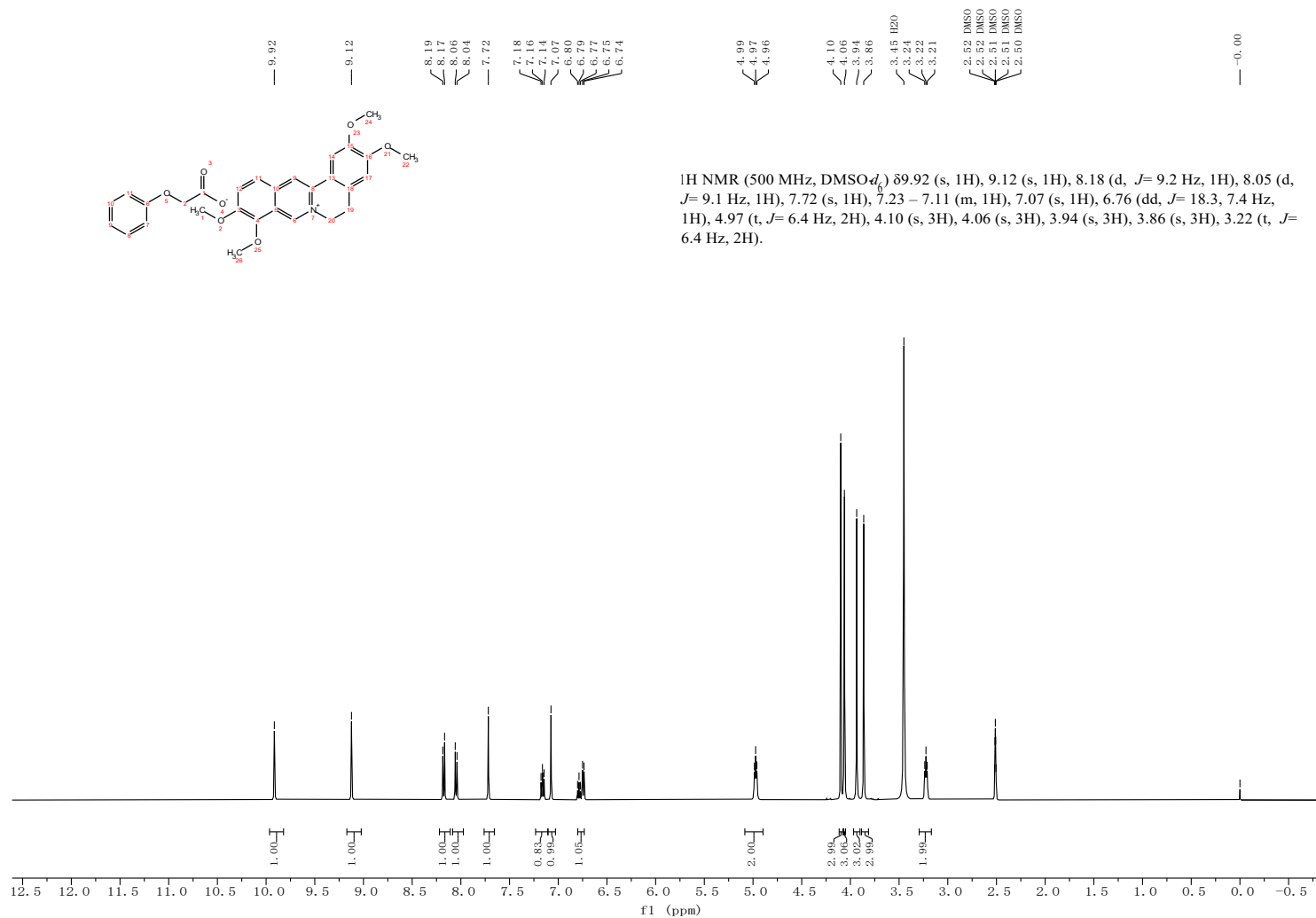


Fig. S38 ¹H NMR (500 MHz; DMSO-*d*₆; Me₄Si) of PIL-1 (2-phenoxyacetate 2,3,9,10-tetramethoxy-5,6-dihydroisoquinolino[3,2-a]isoquinolin-7-ium)

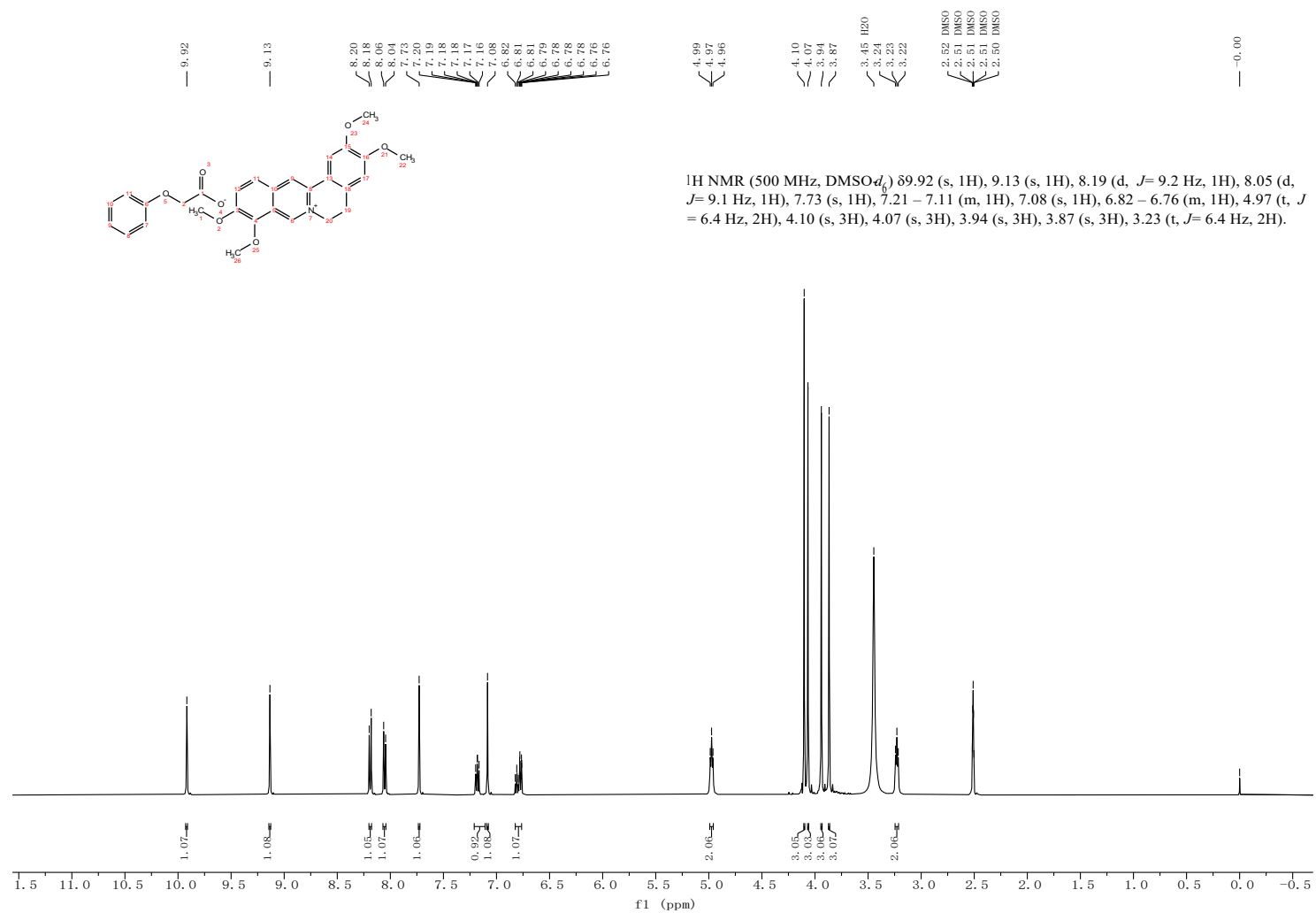


Fig. S39 ¹H NMR (500 MHz; DMSO-d₆; Me₄Si) of PIL-1 after volatility test

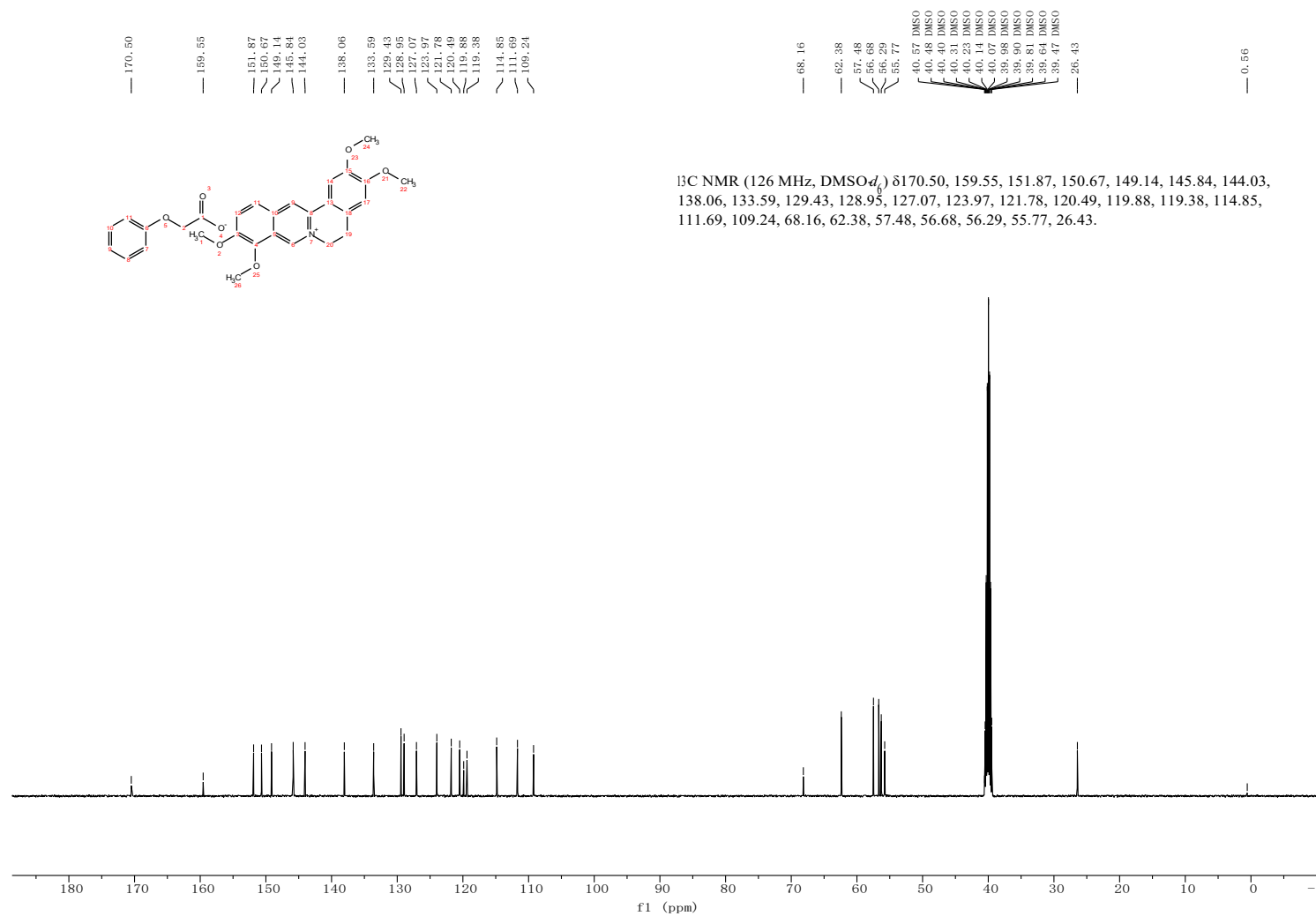


Fig. S40 ^{13}C NMR (126 MHz; DMSO-d_6 ; Me_4Si) of PIL-1 (2-phenoxyacetate 2,3,9,10-tetramethoxy-5,6-dihydroisoquinolino[3,2-a]isoquinolin-7-ium)

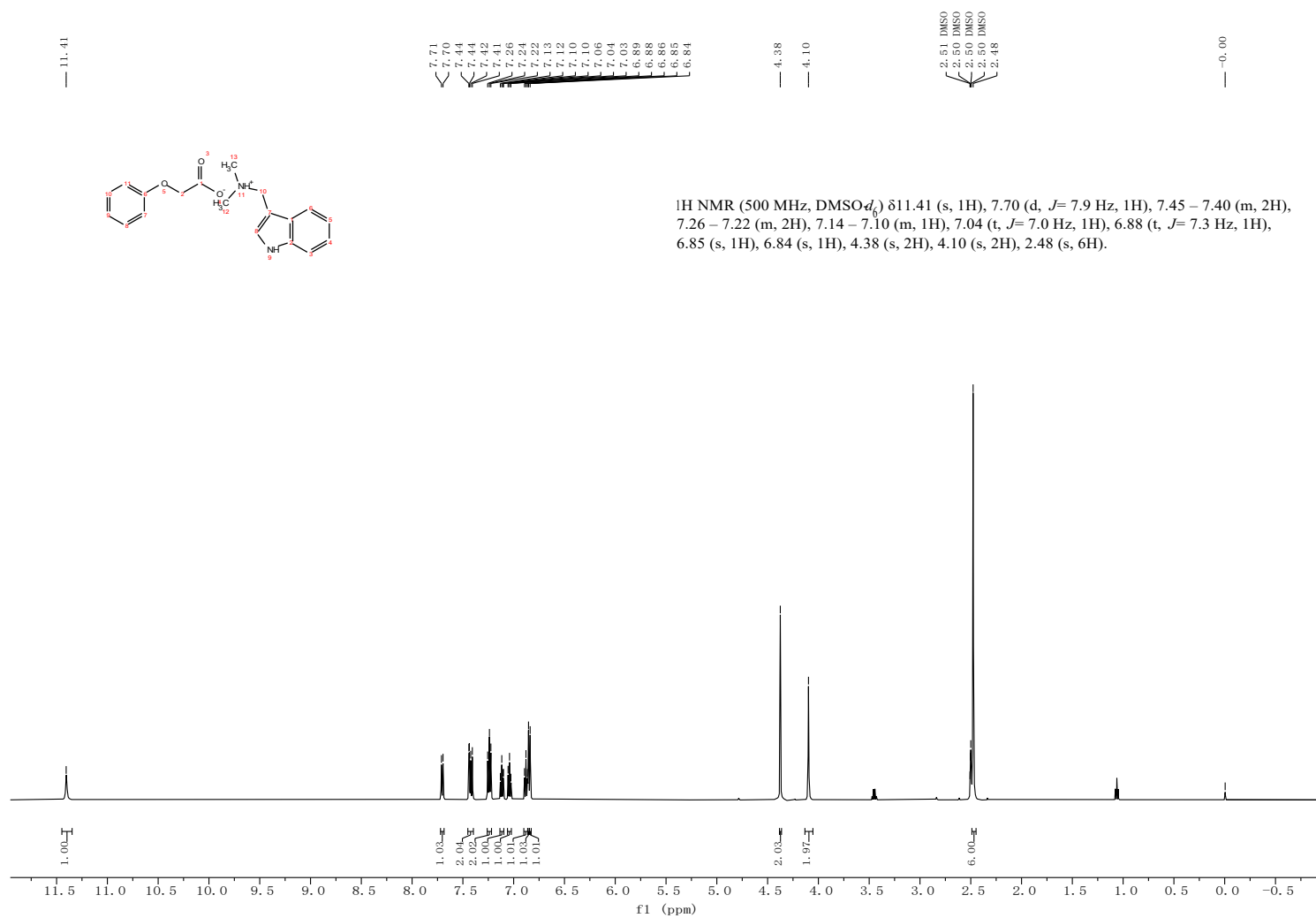


Fig. S41 ¹H NMR (500 MHz; DMSO-*d*₆; Me₄Si) of PIL-2 (2-phenoxyacetate 4,6-dimethyl-N-phenylpyrimidin-2-aminium)

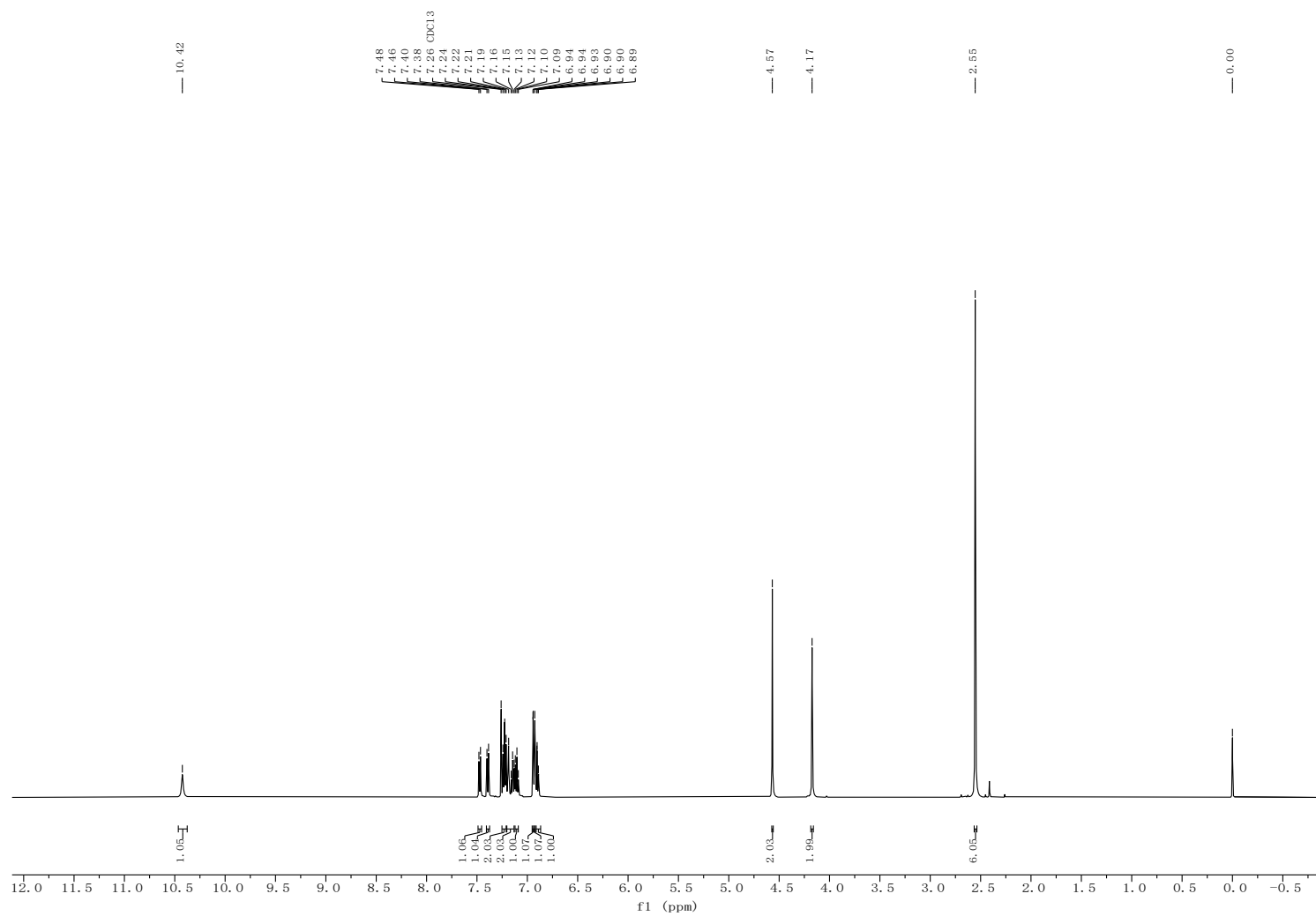


Fig. S42 ¹H NMR (500 MHz; CDCl₃; Me₄Si) of PIL-2 after volatility test

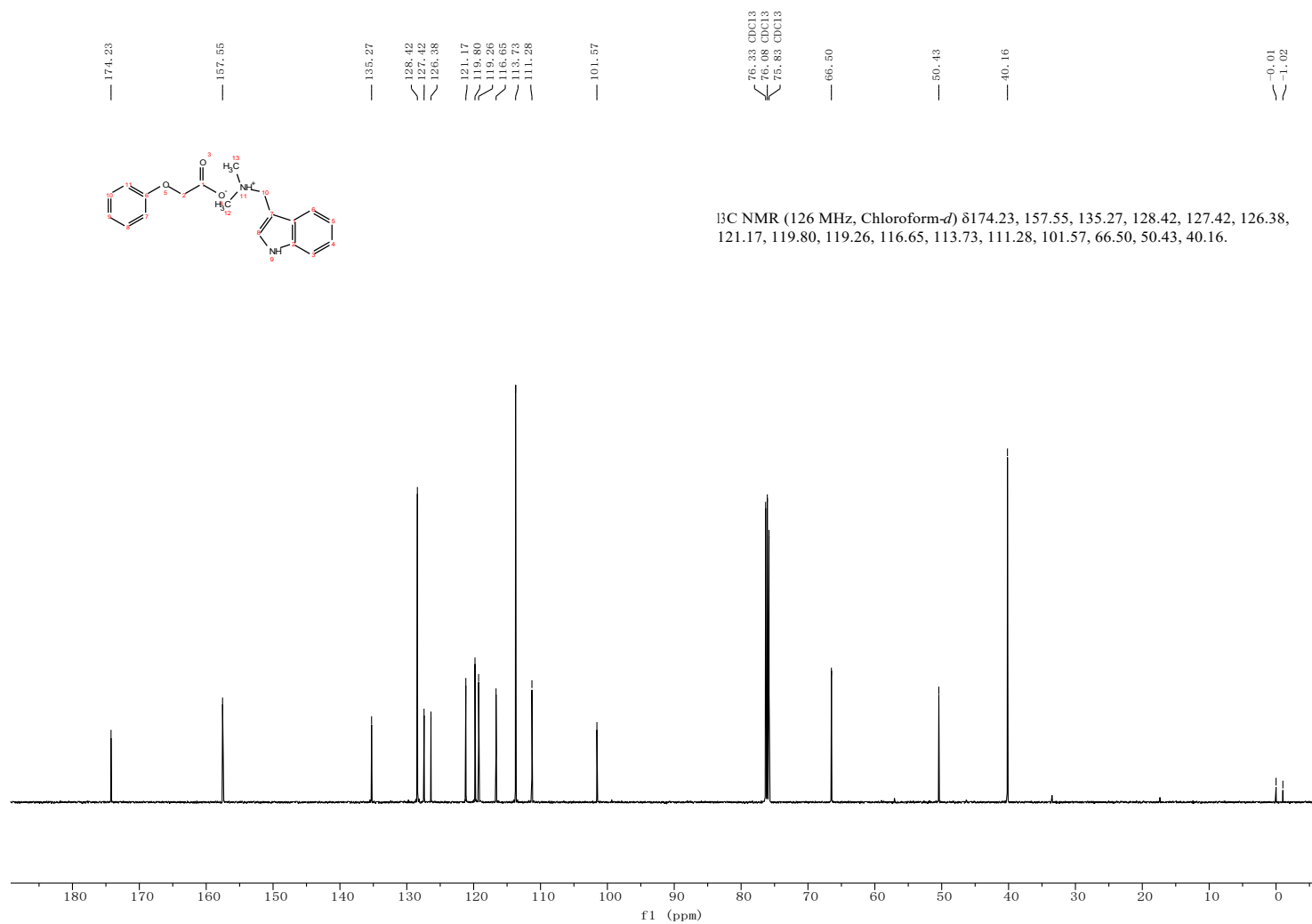


Fig. S43 ¹³C NMR (126 MHz; CDCl₃; Me₄Si) of PIL-2 (2-phenoxyacetate 1-(1H-indol-3-yl)-N,N-dimethylmethanaminium)

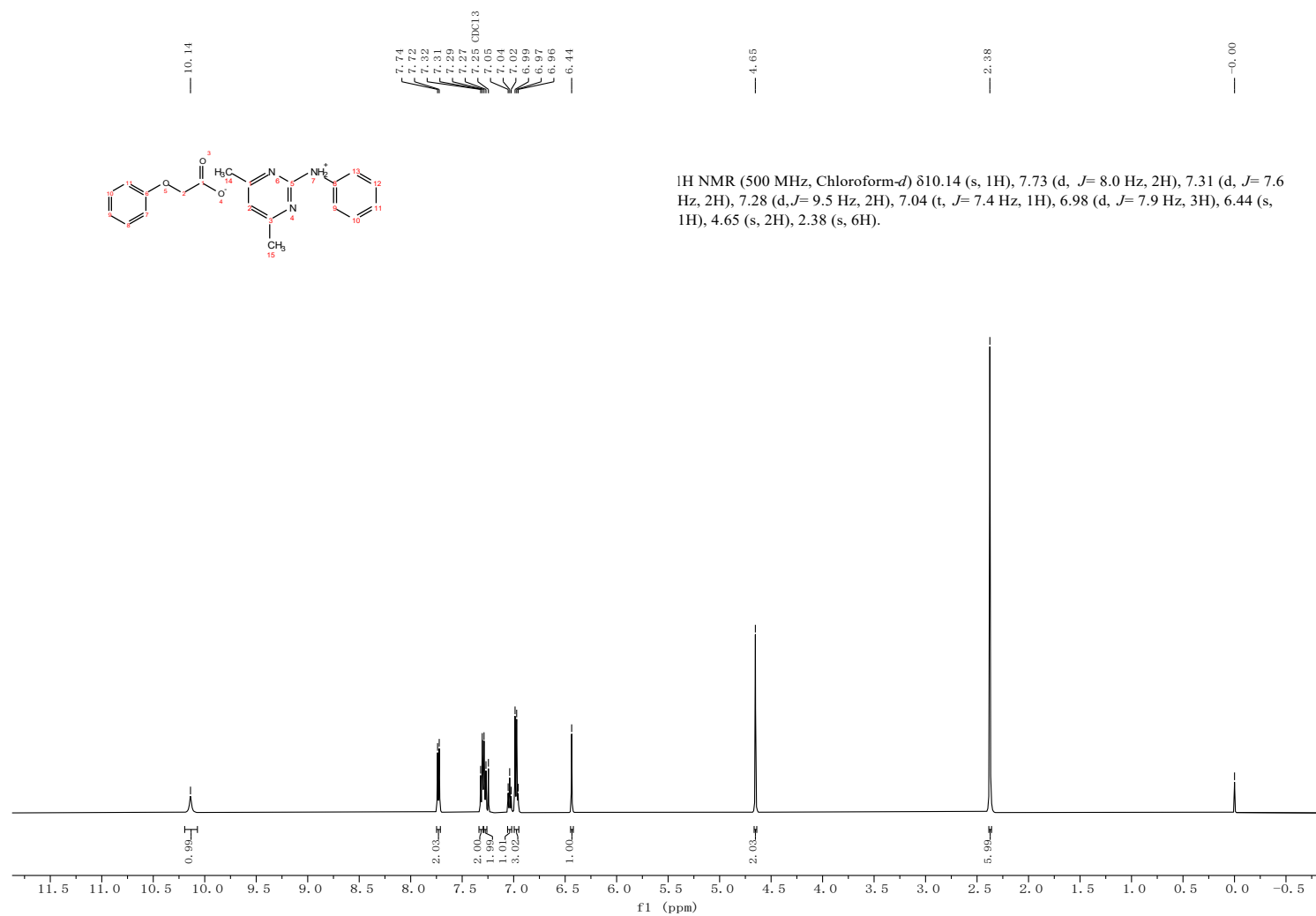


Fig. S44 ¹H NMR (500 MHz; CDCl₃; Me₄Si) of PIL-3 (2-phenoxyacetate 4,6-dimethyl-N-phenylpyrimidin-2-aminium)

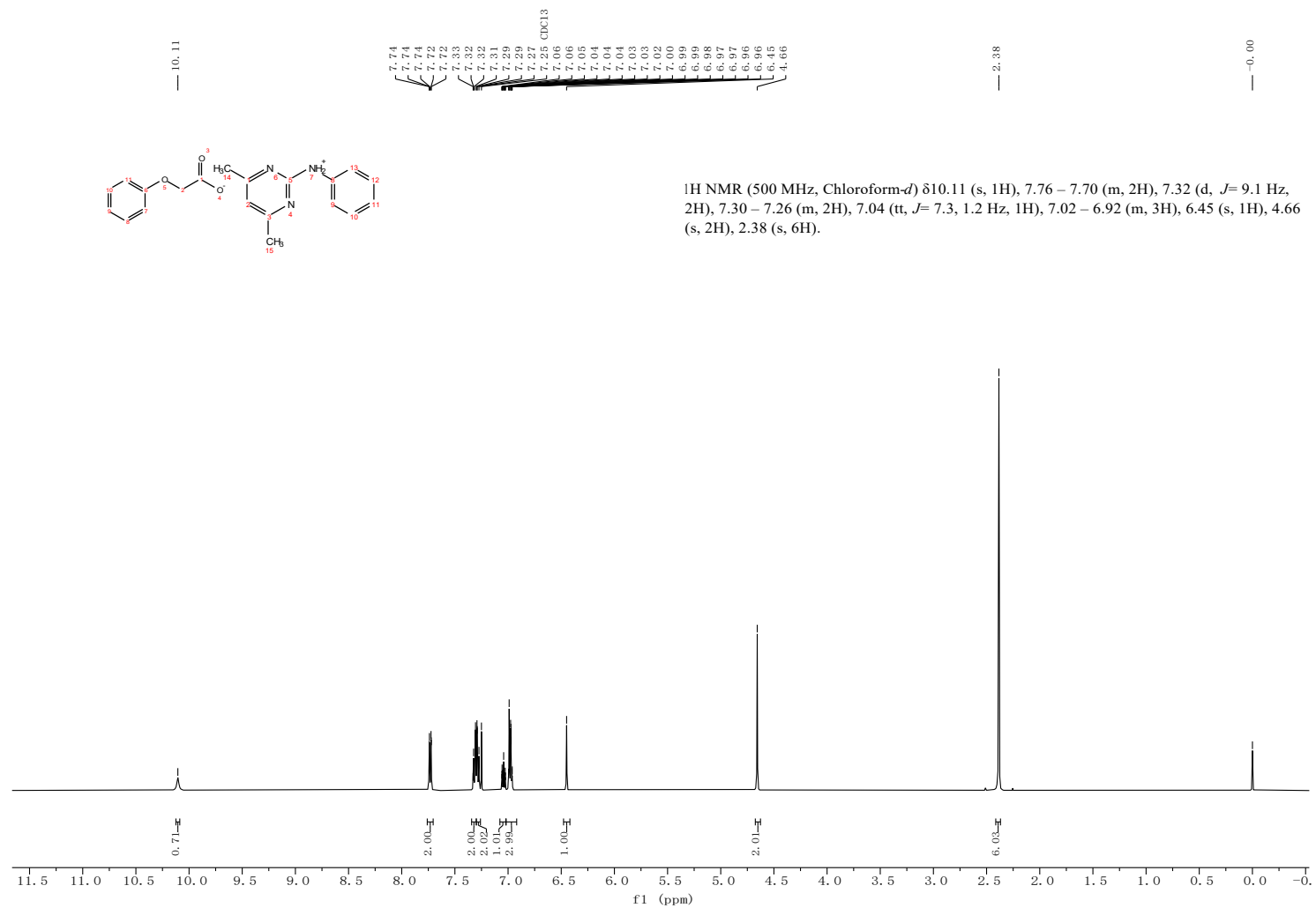


Fig. S45 ¹H NMR (500 MHz; CDCl₃; Me₄Si) of PIL-3 after volatility test

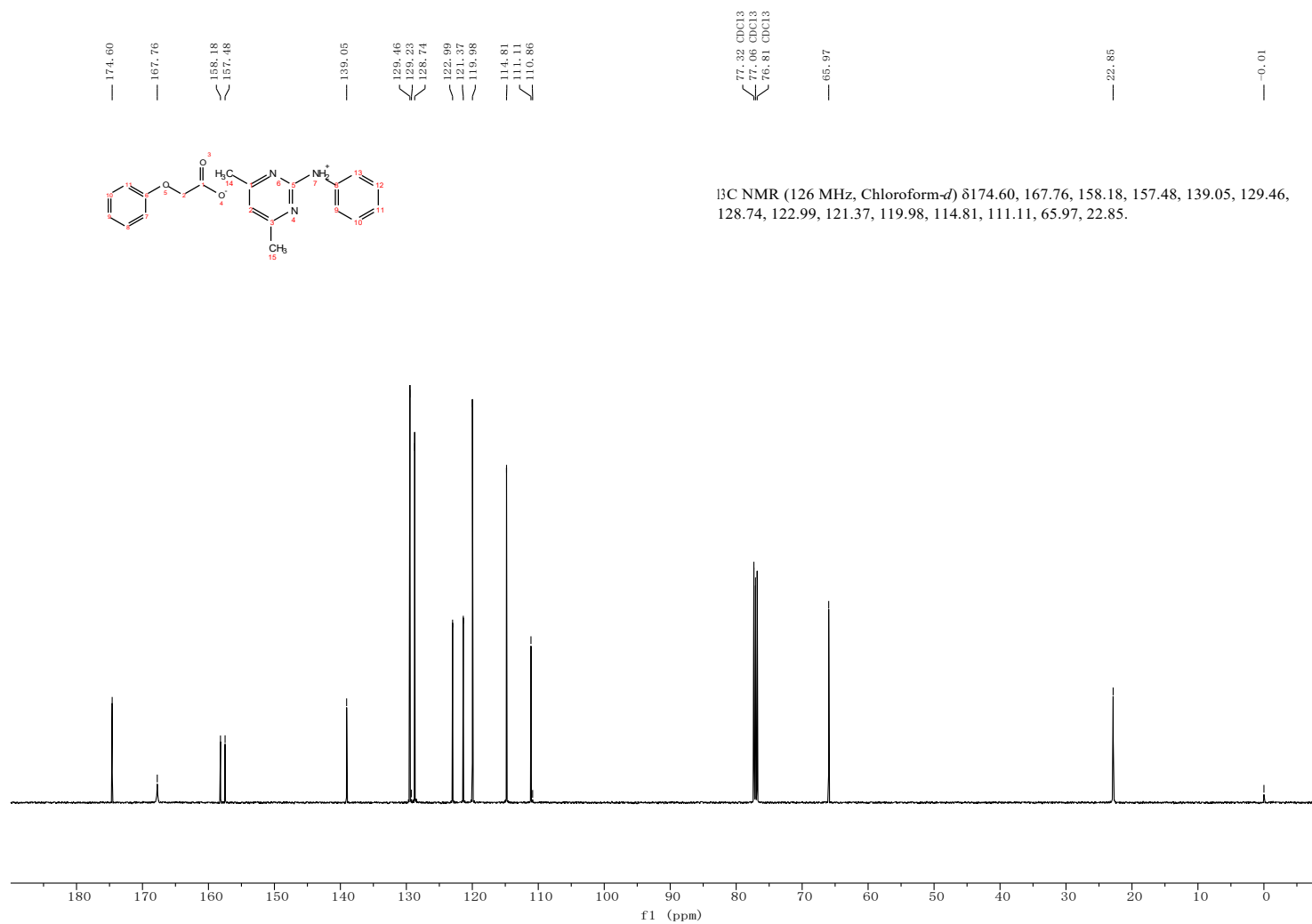


Fig. S46 ¹³C NMR (126 MHz; CDCl₃; Me₄Si) of PIL-3 (2-phenoxyacetate 4,6-dimethyl-N-phenylpyrimidin-2-aminium)

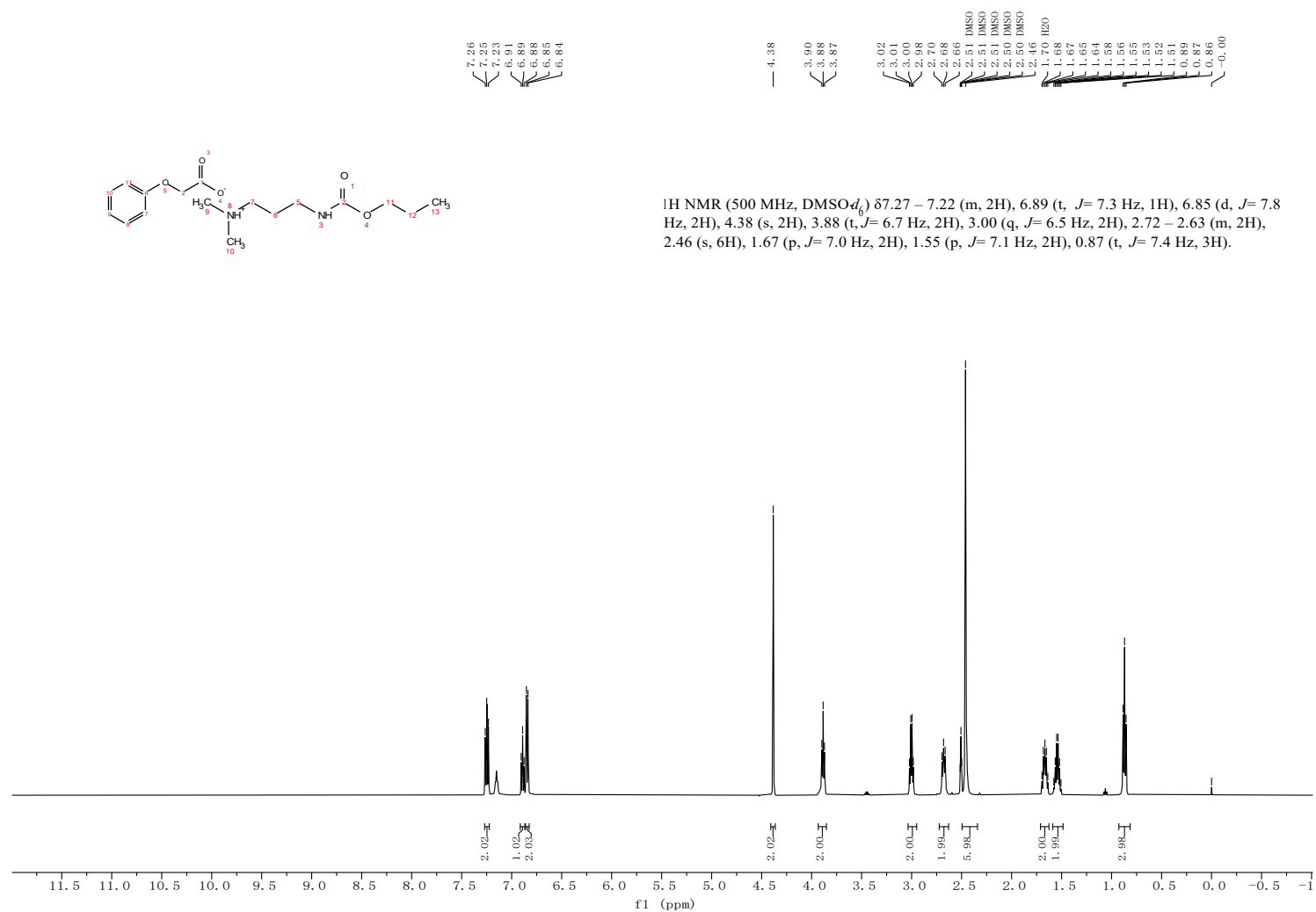


Fig. S47 ¹H NMR (500 MHz; DMSO-d₆; Me4Si) of PIL-4 (2-phenoxyacetate N,N-dimethyl-3-((propoxycarbonyl)amino)propan-1-aminium)

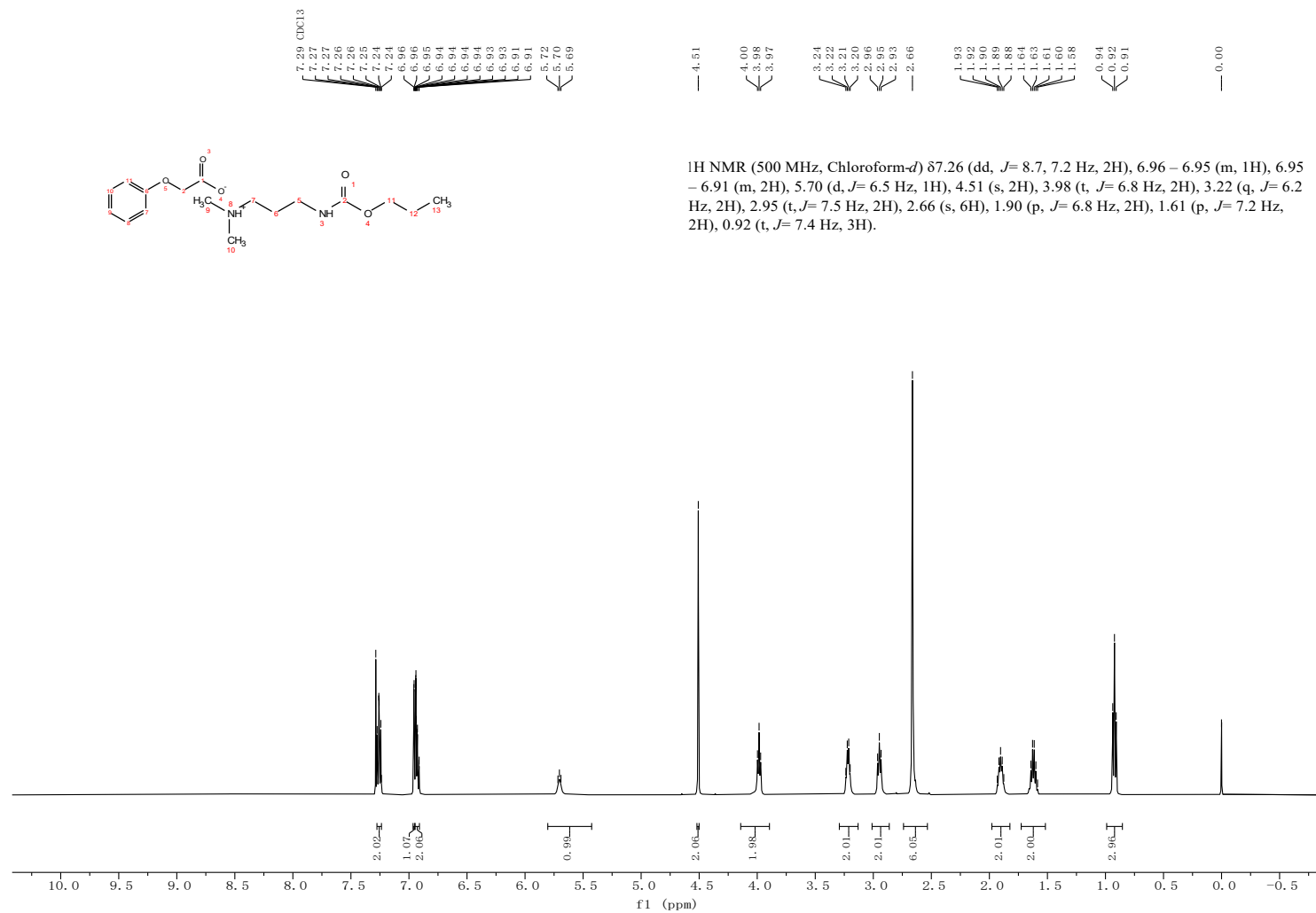


Fig. S48 ¹H NMR (500 MHz; CDCl₃; Me₄Si) of PIL-4 after volatility test

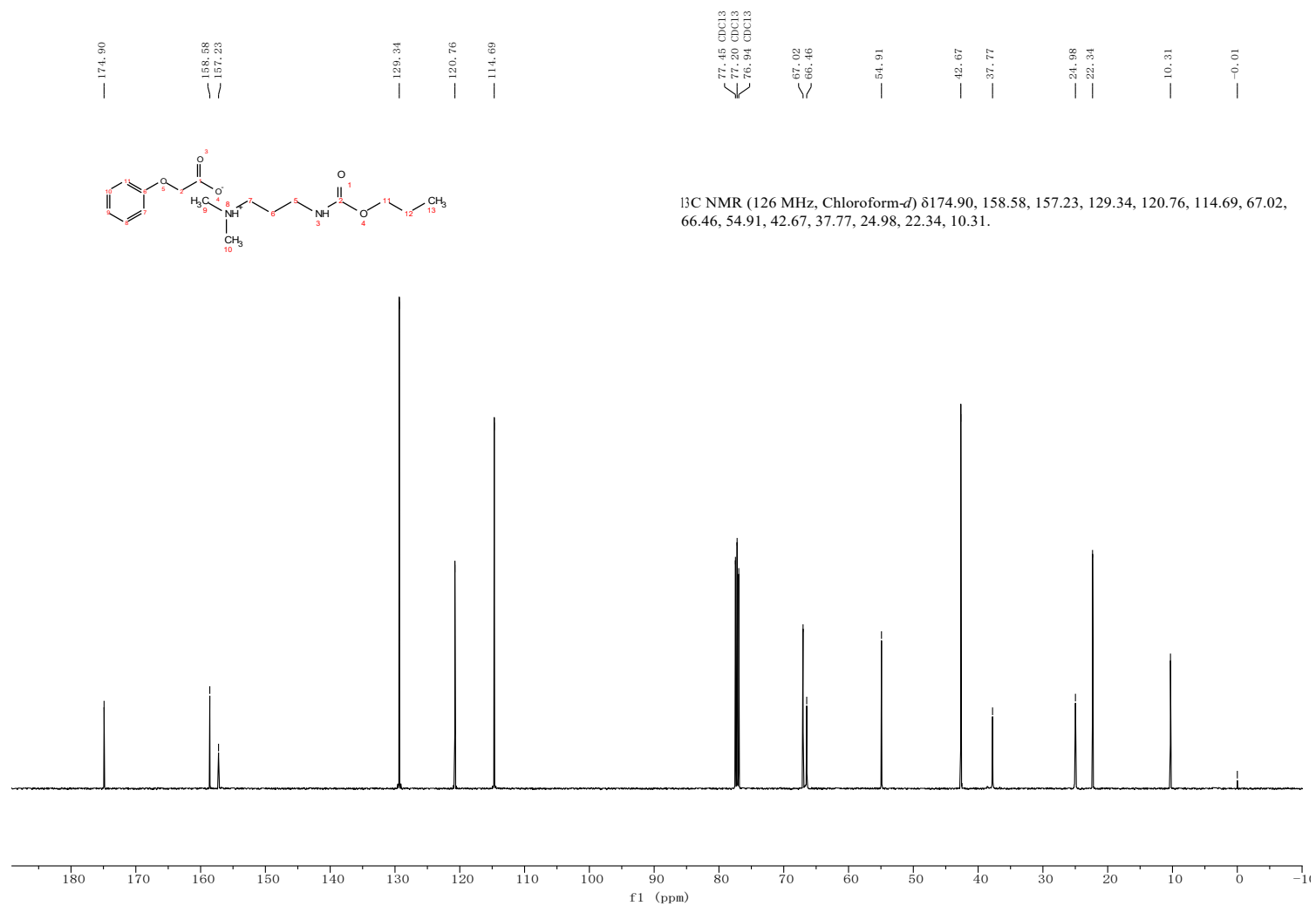


Fig. S49 ¹³C NMR (126 MHz; CDCl₃; Me₄Si) of PIL-4 (2-phenoxyacetate N,N-dimethyl-3-((propoxycarbonyl)amino)propan-1-aminium)